ARMY RESEARCH LABORATORY

A Geometric Framework for the Kinematics of Crystals With Defects

by John D. Clayton, Douglas J. Bammann, and David L. McDowell

ARL-RP-119 February 2006

A reprint from *Philosophical Magazine*, vol. 85, nos. 33–35, pp. 3983–4010, 21 November–11 December 2005.

NOTICES

Disclaimers

The findings in this report are not to be construed as an official Department of the Army position unless so designated by other authorized documents.

Citation of manufacturer's or trade names does not constitute an official endorsement or approval of the use thereof.

Destroy this report when it is no longer needed. Do not return it to the originator.

Army Research Laboratory
Aberdeen Proving Ground, MD 21005-5066

ARL-RP-119 **February 2006**

A Geometric Framework for the Kinematics of Crystals With Defects

John D. Clayton
Weapons and Materials Research Directorate, ARL

Douglas J. Bammann
Sandia National Laboratories

David L. McDowell
Georgia Institute of Technology

A reprint from *Philosophical Magazine*, vol. 85, nos. 33–35, pp. 3983–4010, 21 November–11 December 2005.

REPORT DOCUMENTATION PAGE

Form Approved
OMB No. 0704-0188

1. REPORT DATE *(DD-MM-YYYY)*	2. REPORT TYPE	3. DATES COVERED (From - To)
February 2006	Reprint	1 January 2003–1 January 2006

4. TITLE AND SUBTITLE
A Geometric Framework for the Kinematics of Crystals With Defects

5a. CONTRACT NUMBER

5b. GRANT NUMBER

5c. PROGRAM ELEMENT NUMBER

6. AUTHOR(S)
John D. Clayton, Douglas J. Bammann,[*] and David L. McDowell[†]

5d. PROJECT NUMBER
1L1622618AH80

5e. TASK NUMBER

5f. WORK UNIT NUMBER

7. PERFORMING ORGANIZATION NAME(S) AND ADDRESS(ES)
U.S. Army Research Laboratory
ATTN: AMSRD-ARL-WM-TD
Aberdeen Proving Ground, MD 21005-5066

8. PERFORMING ORGANIZATION REPORT NUMBER
ARL-RP-119

9. SPONSORING/MONITORING AGENCY NAME(S) AND ADDRESS(ES)

10. SPONSOR/MONITOR'S ACRONYM(S)

11. SPONSOR/MONITOR'S REPORT NUMBER(S)

12. DISTRIBUTION/AVAILABILITY STATEMENT
Approved for public release; distribution is unlimited.

13. SUPPLEMENTARY NOTES
A reprint from *Philosophical Magazine*, vol. 85, nos. 33–35, pp. 3983–4010, 21 November–11 December 2005.
[*]Department of Science-Based Materials Modeling, Sandia National Laboratories, Livermore, CA 94550.
[†]GWW School of Mechanical Engineering, Georgia Institute of Technology, Atlanta, GA 30332-0405.

14. ABSTRACT
Presented is a general theoretical framework capable of describing the finite deformation kinematics of several classes of defects prevalent in metallic crystals. Our treatment relies upon powerful tools from differential geometry, including linear connections and covariant differentiation, torsion, curvature, and anholonomic spaces. A length scale dependent, three-term multiplicative decomposition of the deformation gradient is suggested, with terms representing recoverable elasticity, residual lattice deformation due to defect fields, and plastic deformation resulting from defect fluxes. Also proposed is an additional micromorphic variable representing additional degrees-of-freedom associated with rotational lattice defects (i.e. disclinations), point defects, and, most generally, Somigliana dislocations. We illustrate how particular implementations of our general framework encompass notable theories from the literature and classify particular versions of the framework via geometric terminology.

15. SUBJECT TERMS
crystal plasticity, dislocations, disclinations, lattice defects, multiscale models

16. SECURITY CLASSIFICATION OF:			17. LIMITATION OF ABSTRACT	18. NUMBER OF PAGES	19a. NAME OF RESPONSIBLE PERSON
a. REPORT	b. ABSTRACT	c. THIS PAGE			John D. Clayton
UNCLASSIFIED	UNCLASSIFIED	UNCLASSIFIED	UL	34	19b. TELEPHONE NUMBER (*Include area code*) 410-306-0975

Philosophical Magazine,
Vol. 85, Nos. 33–35, 21 Nov.–11 Dec. 2005, 3983–4010

Taylor & Francis
Taylor & Francis Group

A geometric framework for the kinematics of crystals with defects

J. D. CLAYTON*†, D. J. BAMMANN‡ and D. L. McDOWELL§

†Impact Physics Branch, US Army Research Laboratory,
Aberdeen Proving Ground, MD 21005-5069, USA
‡Department of Science-Based Materials Modeling,
Sandia National Laboratories, Livermore, CA 94550, USA
§GWW School of Mechanical Engineering, Georgia Institute of Technology,
Atlanta, GA 30332-0405, USA

(*Received 20 April 2004; in final form 7 February 2005*)

Presented is a general theoretical framework capable of describing the finite deformation kinematics of several classes of defects prevalent in metallic crystals. Our treatment relies upon powerful tools from differential geometry, including linear connections and covariant differentiation, torsion, curvature and anholonomic spaces. A length scale dependent, three-term multiplicative decomposition of the deformation gradient is suggested, with terms representing recoverable elasticity, residual lattice deformation due to defect fields, and plastic deformation resulting from defect fluxes. Also proposed is an additional micromorphic variable representing additional degrees-of-freedom associated with rotational lattice defects (i.e. disclinations), point defects, and most generally, Somigliana dislocations. We illustrate how particular implementations of our general framework encompass notable theories from the literature and classify particular versions of the framework via geometric terminology.

1. Motivation and background

Methods from geometry on differentiable manifolds have come to the fore in recent years for describing the kinematics of elastoplasticity [1–9]. An understanding of the kinematics of defective crystals is central to constructing arguments related to nonlocal or gradient theories introducing scale effects in the description. As such, the primary objective of the present work is to provide a unified framework encapsulating the kinematics of crystalline incompatibilities whose descriptions give rise to higher-order gradient continuum plasticity models. Our scope is restricted to *kinematics* of defects; for complementary treatments of material forces, the reader is referred to works by Eshelby [10, 11], Nabarro [12], Kröner [13], Maugin [1–3] and Gurtin [14].

The two-term multiplicative decomposition of the deformation gradient, $\mathbf{F} = \mathbf{F}^{\mathbf{e}}\mathbf{F}^{\mathbf{p}}$, was proposed by Bilby *et al.* [15] and Kröner [16] for modeling the

*Corresponding author. Email: jclayton@arl.army.mil

Philosophical Magazine
ISSN 1478–6435 print/ISSN 1478–6443 online
http://www.tandf.co.uk/journals
DOI: 10.1080/14786430500363312

deformation of single crystals within the framework of continuously distributed dislocations. In the theory of Bilby *et al*. [15], $\mathbf{F}, \mathbf{F}^{\mathbf{e}}$, and $\mathbf{F}^{\mathbf{p}}$ are described as the 'shape deformation', the 'lattice deformation', and the 'dislocation deformation', respectively. The existence of a generally incompatible, relaxed intermediate configuration was described in the years prior, for example, by Eckart [17], Kondo [18], Bilby *et al*. [19] and Eshelby [11]. Kondo [18] and Bilby *et al*. [19] are usually credited with discovering the relationship between the density of continuously distributed dislocations and Cartan's torsion tensor of the 'crystal connection', which we will see may be defined in terms of a spatial gradient of the (inverse) lattice deformation. The geometry induced by the crystal connection is said to possess a 'distant parallelism' or a 'teleparallelism' [20], and exhibits the special property that covariant derivatives taken with respect to this connection of spatially constant intermediate configuration slip vectors vanish. The null curvature property of the crystal connection (*cf*. [21]), together with knowledge of its torsion and either the covariant plastic or elastic strain tensor is sufficient to uniquely specify the relaxed intermediate configuration, as demonstrated by Le and Stumpf [4]. Le and Stumpf [5] and Steinmann [6] also provide geometric viewpoints of the kinematics of higher-gradient finite elastoplasticity of crystals with defects. Also of interest is the description of Noll [21] admitting multiple reference configurations. Rajagopal and Srinivasa [22] developed a framework capable of characterizing evolving elastic symmetry in a wide class of fluids and solids, wherein the deformation is described as the evolution of a family of 'natural configurations'. Cermelli and Gurtin [23] examined the kinematics of geometrically necessary dislocations from the perspective of multiplicative elastoplasticity with plastic deformation characterized by shearing on discrete slip systems. Other noteworthy efforts employing differential geometry to describe generalized continua include the manifold-based treatment of Marsden *et al*. [24] and methods founded upon gauge theories and/or exterior calculus [7, 25, 26].

Since dislocations associated with the crystal connection are required to sustain compatibility of the total deformation and may induce local residual stresses within the crystal, they are often labeled 'geometrically necessary' dislocations in the sense of Ashby [27]. This is in contrast to the 'absolute' dislocations [28, 29] or 'statistically stored' dislocations [27] that sustain homogeneous plastic deformation. Lardner [28] showed that vanishing of the torsion tensor of the crystal connection corresponds to vanishing of excess dislocations of the same sign. Nye [30] associated a dislocation density tensor with the gradient of lattice rotation, i.e. the stress-free lattice curvature. Kroupa [31] proposed a loop density tensor for describing the contributions of dislocation loops to the plastic distortion field and induced internal stresses. Kröner [32, 33] suggested inclusion of various statistical moments of dislocation distributions in theories of work hardening. Grain boundary, surface, and interface dislocations have also been investigated from the geometric viewpoint [34–38].

Kondo [18, 39, 40] proposed more general frameworks for yielding and plastic deformation allowing nonzero Riemann–Christoffel curvature associated with a connection different from the crystal connection. Kondo's frameworks admit different non-unique anholonomic (i.e. incompatible) intermediate configurations, or 'tearings' in his terminology, for the same crystal. These configurations differ

from the unique intermediate configuration favored by Bilby *et al*. [19], for which the curvature of the crystal connection vanishes and teleparallelism is preserved. Kondo [40] associated the nonzero curvature with the presence of 'rotational anomalies' in the lattice, which could be interpreted as disclinations [41, 42]. Connections admitting non-vanishing curvature tensors have since been used by many for modeling disclinations in Bravais lattices [43–48]. Rotational defects falling under the general category of Somigliana dislocations (*cf*. [10, 11, 49, 50]) were addressed in terms of a path-dependent integral of the non-vanishing curvature tensor by Pęcherski [51, 52]. Non-metric connections admitting 'extra-matter' defects (e.g. interstitial atoms, vacancies, and other point defects) were introduced in continuum theories by Kröner [16, 53, 54], Minagawa [45] and De Wit [48].

The remainder of the present paper is organized as follows. Section 2 defines relevant terminology, followed by mathematical preliminaries in section 3. In section 4, we present our kinematic description at the macro-level, specifically the decomposition of the deformation gradient for a local volume element of crystalline material. Section 5 provides our kinematic description at the micro-level, in terms of an affine connection, possibly non-metric with a potentially non-vanishing curvature tensor. We illustrate throughout sections 4 and 5 how our description encompasses the physics of translational dislocations, disclinations, point defects, and Somigliana dislocations, and we discuss how particular versions of our framework reduce to noteworthy models in prior literature. Key features are summarized in tabular form in section 6.

2. Terminology

Here, we summarize terminology that is often a source of confusion to readers not well-versed in differential geometry and its application to continuum mechanics. The definitions given immediately below are free of notation and hence are somewhat qualitative; in many cases corresponding equations may be found later in the paper, or the reader may elect to consult more extensive sources (e.g. [55–57]).

- *Configuration*. A configuration is defined as a generally time-dependent realization of a body. In finite deformation theories, one often speaks of the 'reference', 'initial', 'undeformed', or 'Lagrangian' configuration, usually and somewhat arbitrarily taken at zero time. Similarly, the 'spatial', 'current', 'deformed', or 'Eulerian' configuration is usually taken at the current time. These two configurations are assumed to be *holonomic* to one another, meaning that current coordinates can be written as smooth, single-valued functions of reference coordinates, and vice-versa. In contrast, the virtual 'intermediate', 'relaxed', or 'unloaded' configuration of elastoplasticity is often *anholonomic*, since its coordinates cannot always be prescribed as single-valued functions of reference or current coordinates. The reader is referred to Wang and Truesdell [56] for a more in-depth discussion.
- *Metric tensor*. A metric tensor (or simply a 'metric') is a rank 2 covariant tensor that defines the scalar product of contravariant vectors, and consequently, the squared length of a vector. A metric tensor that is both symmetric

and positive definite is called a *Riemannian metric tensor*†; non-Riemannian metrics will not be employed here. Metric tensors perform other consequential functions, such as raising and lowering indices and defining scalar products.

- *Connection*. A linear‡ connection is a rank three construct that defines a covariant derivative of vectors (*cf*. (1)) and tensors of higher rank (4). Alternatively and equivalently, the covariant derivative operation defines the connection coefficients (i.e. Christoffel symbols). See Eisenhart [58] or Boothby [59] for additional perspective.

Note that a particular configuration or space can be assigned more than one connection, just as it can be assigned more than one metric tensor. We can often classify the pair of {configuration, connection} or triad of {configuration, connection, metric tensor} as one or more of the following five types of 'geometric spaces':

(1) *Euclidean space*. For a space to be classified as Euclidean or non-Euclidean, it must include a configuration, a metric tensor, and a connection. A Euclidean space satisfies three requirements: (i) the torsion tensor from the connection vanishes, (ii) the covariant derivative of the metric tensor vanishes, and (iii) the Riemann–Christoffel curvature tensor from the connection coefficients vanishes. A Euclidean n-space permits at each location a transformation from local coordinates to a global n-dimensional Cartesian coordinate system. In continuum mechanics, both the reference and current configurations are typically viewed as three-dimensional Euclidean spaces, with the motion acting as a *diffeomorphism* (i.e. a differentiable *homeomorphism*, or a differentiable one-to-one, invertible mapping) between these two configurations [61]. Notice the distinction between *Euclidean* and *Cartesian*: the former (e.g. spherical coordinates in three dimensions) admits a global transformation to the latter (e.g. three constant and orthonormal basis vectors).

(2) *Anholonomic space*. An anholonomic space is regarded as a configuration defined by a non-integrable, two-point deformation map. In multiplicative plasticity, since $\mathbf{F}^{\mathbf{e}-1}$ and $\mathbf{F}^{\mathbf{p}}$ are generally non-integrable or 'anholonomic' functions of current and reference coordinates, respectively, the corresponding intermediate configuration is generally anholonomic. Coordinate functions on such an anholonomic space are necessarily discontinuous, multi-valued functions of current or reference configuration 'holonomic' coordinates. Anholonomicity is related to Cartan's torsion tensor of a certain connection (i.e. the crystal connection) constructed from the lattice deformation in our theory, as discussed in section 5.1 (see equation (21)). Anholonomic coordinates are discussed at length by Schouten [55].

† A non-Riemannian metric tensor would not be positive-definite. Such metrics arise in more generalized geometries such as Finlser spaces, an example of which is Minkowski's spacetime (*cf*. Rund [60]). Metrics are symmetric by definition.

‡ In the present work we focus on *linear* (also called *affine*) connections, which strictly obey (1). *Nonlinear* connections arise in more generalized spaces such as Finsler manifolds [60] and will not be dealt with here.

(3) *Cartan space*. A configuration with a connection admitting a non-vanishing Cartan's torsion tensor is labeled a 'Cartan' space, sometimes called a 'non-symmetric' space. We need only consider the pair {configuration, connection} to label a space as Cartan or non-Cartan.
(4) *Riemannian space*. For a space to be labeled as 'Riemannian' or 'non-Riemannian' it must include the pair {configuration, connection} — a metric is not needed for our designation. A Riemannian space is defined here as a configuration with connection coefficients whose components yield a nonzero Riemann–Christoffel curvature tensor. A space with a non-vanishing curvature is non-Euclidean: for example, a global 2D Cartesian coordinate system cannot be used to parameterize a shell unless the shell is flat. Conversely, a space with vanishing curvature is 'non-Riemannian', and the connection is said to be 'integrable'.
(5) *Non-metric space*. For one to label a generalized space as 'metric' or 'non-metric' the configuration must be assigned both a linear connection and a metric tensor; we must examine the trio of {configuration, connection, metric tensor}. In a non-metric space, the covariant derivative of the metric tensor taken with respect to the connection is nonzero.

The above terminology is not fully consistent in the literature [6, 19, 21, 40, 55, 57]. We have attempted to use terminology appearing most frequently and logically for describing crystals.

3. Mathematical preliminaries

Reviewed next are fundamental geometric concepts. Definitions are given first, followed by a discussion of strain compatibility and anholonomic coordinates. For more in-depth treatments, the reader is referred Schouten [55], Wang and Truesdell [56] and Marsden and Hughes [57]. Boldface type is used for vectors and tensors of higher rank, while scalars and components of tensors are written in italics. In order to appeal to a broad audience (e.g. engineers, physicists, and mathematicians) we often use the index notation favored by earlier differential geometers [55, 58] even though many expressions could be presented more concisely via more modern direct notation of tensor analysis on manifolds and exterior calculus [7, 57].

3.1. *Definitions*

An *n-manifold* is a set M such that for each $P \in M$ there is a subset U of M containing P, and a one-to-one mapping from U onto an open set in $\mathbb{R}^n$ (the n- space of real numbers). Changes in coordinates over coincident regions are assumed to be infinitely differentiable if the manifold is smooth. For the present discussion, we introduce a smooth manifold B_0, which we associate with the reference configuration of a body in the terminology of finite deformation continuum mechanics. Manifold B_0 is parameterized by coordinates X^A $(A = 1, 2, 3)$, with the *tangent space* at each $\mathbf{X}$ spanned by the natural basis vectors $\mathbf{G}_A \equiv \partial_A \mathbf{X}$, where $\partial_A \equiv \partial/\partial X^A$. The ensemble of local tangent spaces of B_0, or *tangent bundle*, is written TB_0.

The metric tensor corresponding to natural basis vectors on B_0 is denoted $\mathbf{G}$, where $G_{AB} = \mathbf{G}_A \cdot \mathbf{G}_B$.

A *linear connection* (also often called an *affine connection*) on a manifold B_0 induces an operation ∇ that assigns to two vector *fields* $\mathbf{V}, \mathbf{W} \in TB_0$ a third vector field $\nabla_{\mathbf{V}}\mathbf{W} \in TB_0$, called the *covariant derivative* of $\mathbf{W}$ along $\mathbf{V}$, such that

$$\begin{aligned} &\text{(i)} \quad \nabla_{\mathbf{V}}\mathbf{W} \text{ is linear in both } \mathbf{W} \text{ and } \mathbf{V};\\ &\text{(ii)} \quad \nabla_{f\mathbf{V}}\mathbf{W} = f\nabla_{\mathbf{V}}\mathbf{W} \text{ for scalar functions } f;\\ &\text{(iii)} \quad \nabla_{\mathbf{V}}(f\mathbf{W}) = f\nabla_{\mathbf{V}}\mathbf{W} + \mathbf{V}(\mathbf{D}f)\mathbf{W}. \end{aligned} \tag{1}$$

In (iii) above, $\mathbf{V}(\mathbf{D}f) = V^A \partial_A f$. The *Christoffel symbols* (or *connection coefficients*) $\Gamma^{\cdot\cdot A}_{BC}$ of a connection ∇ on B_0 are defined on a coordinate system X^A, with holonomic basis $\{\mathbf{G}_A\}$, by

$$\Gamma^{\cdot\cdot A}_{BC}\mathbf{G}_A = \nabla_{\mathbf{G}_B}\mathbf{G}_C. \tag{2}$$

Using equations (1) and (2), the covariant derivative of $\mathbf{W}$ along $\mathbf{V}$ is written as

$$\nabla_{\mathbf{V}}\mathbf{W} = \left(V^B \partial_B W^A + \Gamma^{\cdot\cdot A}_{BC} V^B W^C\right)\mathbf{G}_A. \tag{3}$$

An affine connection on the tangent bundle TB_0 defines parallel transport of vectors on different tangent spaces in TB_0, such that vectors in different tangent spaces may be compared, permitting calculation of the change of constituent vectors of a vector field over the entire tangent bundle. A vector is said to undergo *parallel transport* (with respect to a connection with covariant derivative ∇) along paths for which its covariant derivative vanishes. For example, a vector $\mathbf{W}$ is considered to be "parallel" along a curve $\lambda(t)$ if $\nabla_{\mathbf{V}}\mathbf{W} = \mathbf{0}$, where $\mathbf{V} = \partial\lambda/\partial t$ is the tangent vector to the curve at the current value of parameter t.

The covariant derivative is applied to $\left\{{N \atop M}\right\}$ tensor fields as [55]:

$$\begin{aligned} \nabla_N A(X)^{A\ldots F}_{G\ldots M} = {} & \partial_N A^{A\ldots F}_{G\ldots M} + \Gamma^{\cdot\cdot A}_{NR} A^{RB\ldots F}_{G\ldots M} + \cdots + \Gamma^{\cdot\cdot F}_{NR} A^{A\ldots ER}_{G\ldots M} \\ & - \Gamma^{\cdot\cdot R}_{NG} A^{A\ldots F}_{RH\ldots M} - \cdots - \Gamma^{\cdot\cdot R}_{NM} A^{A\ldots F}_{G\ldots LR}, \end{aligned} \tag{4}$$

where we have placed the index of covariant differentiation as a subscript immediately following the ∇-operator. Analogous to parallel transport of vectors, a tensor is parallel transported along a curve if its covariant derivative vanishes as the tensor is 'dragged' along the curve.

The *torsion* tensor $\mathbf{T}$ of a connection is defined by

$$\mathbf{T}(\mathbf{V}, \mathbf{W}) \equiv \nabla_{\mathbf{V}}\mathbf{W} - \nabla_{\mathbf{W}}\mathbf{V} - [\mathbf{V}, \mathbf{W}], \tag{5}$$

where the *Lie bracket* of vector fields $\mathbf{V}$ and $\mathbf{W}$ on TB_0 is given by

$$[\mathbf{V}, \mathbf{W}] = \left(V^B \partial_B W^A - W^B \partial_B V^A\right)\mathbf{G}_A. \tag{6}$$

Using Equations (3), (5) and (6), the coordinate representation of the torsion tensor is found as

$$\mathbf{T} = \left(\Gamma^{\cdot\cdot A}_{BC} - \Gamma^{\cdot\cdot A}_{CB}\right)\mathbf{G}_A \otimes \mathbf{G}^B \otimes \mathbf{G}^C = 2\Gamma^{\cdot\cdot A}_{[BC]}\mathbf{G}_A \otimes \mathbf{G}^B \otimes \mathbf{G}^C, \tag{7}$$

where indices enclosed in brackets $[\cdot]$ are anti-symmetrized, i.e. $2A_{[AB]} = A_{AB} - A_{BA}$, and $\otimes$ is the outer product. The torsion tensor of a linear connection is often called *Cartan's torsion*, by association with geometer E. Cartan [62]. A connection with vanishing torsion is said to be *symmetric*. For a smooth manifold B_0 with Riemannian metric $\mathbf{G}$, there is a unique affine connection, which we label now $\overset{\mathbf{G}}{\nabla}$, on B_0 that is torsion-free ($\overset{\mathbf{G}}{\mathbf{T}} = \mathbf{0}$) and for which parallel transport preserves dot products of vectors, i.e. $\overset{\mathbf{G}}{\nabla}\mathbf{G} = \mathbf{0}$. It is called the *Levi-Civita connection* [57] or the *Riemannian connection* [63]. The connection coefficients of the covariant derivative $\overset{\mathbf{G}}{\nabla}$ are defined by

$$\overset{\mathbf{G}}{\mathbf{\Gamma}} \equiv \frac{1}{2} G^{AB}(\partial_D G_{CB} + \partial_C G_{DB} - \partial_B G_{DC})\mathbf{G}_A \otimes \mathbf{G}^C \otimes \mathbf{G}^D. \tag{8}$$

A connection yielding a null covariant derivative of the metric tensor is called a *metric connection*. The Levi–Civita connection of (8) is metric. Note that in Cartesian coordinates, $G_{AB} = \delta_{AB} = \text{constant}$, meaning that the Christoffel symbols from G_{AB} vanish by (8).

The *Riemann–Christoffel curvature tensor* associated with an arbitrary linear connection with covariant derivative ∇ on B_0 is a $\left\{\begin{smallmatrix}1\\3\end{smallmatrix}\right\}$ tensor satisfying [57]

$$\mathbf{R}(\boldsymbol{\alpha}, \mathbf{W}_1, \mathbf{W}_2, \mathbf{W}_3) = \boldsymbol{\alpha}(\nabla_{\mathbf{W}_1}\nabla_{\mathbf{W}_2}\mathbf{W}_3 - \nabla_{\mathbf{W}_2}\nabla_{\mathbf{W}_1}\mathbf{W}_3 - \nabla_{[\mathbf{W}_1, \mathbf{W}_2]}\mathbf{W}_3), \tag{9}$$

where $\boldsymbol{\alpha}$ and $\mathbf{W}_i$ denote, respectively, arbitrary *one-forms* (i.e. covariant vectors) and contravariant vectors in configuration B_0. The component representation of $\mathbf{R}$ is given by

$$\mathbf{R} = \left(\partial_C \Gamma^{\cdot\cdot A}_{DB} - \partial_D \Gamma^{\cdot\cdot A}_{CB} + \Gamma^{\cdot\cdot A}_{CE}\Gamma^{\cdot\cdot E}_{DB} - \Gamma^{\cdot\cdot A}_{DE}\Gamma^{\cdot\cdot E}_{CB}\right)\mathbf{G}_A \otimes \mathbf{G}^B \otimes \mathbf{G}^C \otimes \mathbf{G}^D. \tag{10}$$

We denote by $\overset{\mathbf{G}}{\mathbf{R}}$ the curvature tensor formed by inserting the Levi–Civita connection (8) into (10). A geometric space B_0 with metric $\mathbf{G}$ having $\overset{\mathbf{G}}{\mathbf{R}} = \mathbf{0}$ is called *flat*. One may show (*cf.* [55]) that $\overset{\mathbf{G}}{\mathbf{R}} = \mathbf{0}$ if and only if we may assign coordinate bases at each $X \in B_0$ such that $G_{AB} \to \delta_{AB}$; i.e. if and only if B_0 is Euclidean. In fact, $\overset{\mathbf{G}}{\mathbf{R}} = \mathbf{0}$ are compatibility conditions for existence of connection coefficients $\overset{\mathbf{G}}{\mathbf{\Gamma}}$ derived from a Euclidean metric $\mathbf{G}$ via (8).

3.2. *Finite strain compatibility*

Assume that the coordinates X^A covering B_0 undergo a smooth, time-dependent mapping to 'current' coordinates $x^a = \varphi^a(X^A, t)$ spanning B. Current configuration B is parameterized by spatial coordinates x^a ($a = 1, 2, 3$), with the tangent space at each point on B spanned by the natural basis vectors $\mathbf{g}_a \equiv \partial_a \mathbf{x}$. The tangent bundle in the current configuration is TB, and the metric tensor $\mathbf{g}$ corresponding to the natural bases on B has components $g_{ab} = \mathbf{g}_a \cdot \mathbf{g}_b$. The linear tangent map $\mathbf{F} \equiv T\boldsymbol{\varphi}$ is labeled the local *deformation gradient*:

$$\mathbf{F} = F^a_{\cdot A}\mathbf{g}_a \otimes \mathbf{G}^A = \frac{\partial \varphi^a}{\partial X^A}\mathbf{g}_a \otimes \mathbf{G}^A. \tag{11}$$

The right Cauchy–Green deformation tensor is the pull-back of the current configuration metric:

$$\mathbf{C} \equiv \boldsymbol{\varphi}^*(\mathbf{g}) = F^a_{\ .A} g_{ab} F^b_{\ .B} \mathbf{G}^A \otimes \mathbf{G}^B, \tag{12}$$

where $\boldsymbol{\varphi}^*$ denotes the pull-back operation by $\mathbf{F}$ (*cf.* [57]). The strain tensor $\mathbf{C}$ assigns any (infinitesimal) vector $d\mathbf{X} = dX^A \mathbf{G}_A$ the length it obtains after deformation by $\mathbf{F}$, i.e. $\|d\mathbf{x}\| = \|\mathbf{F} d\mathbf{X}\| = \sqrt{\langle \mathbf{C} d\mathbf{X}, d\mathbf{X} \rangle} = \sqrt{C_{AB} dX^A dX^B}$. We introduce a linear connection

$$\overset{\mathbf{C}}{\boldsymbol{\Gamma}} \equiv \frac{1}{2} \left(C^{-1}\right)^{AB} (\partial_D C_{CB} + \partial_C C_{DB} - \partial_B C_{DC}) \mathbf{G}_A \otimes \mathbf{G}^C \otimes \mathbf{G}^D. \tag{13}$$

We then form the curvature $\overset{\mathbf{C}}{\mathbf{R}}$ by substituting the components of $\overset{\mathbf{C}}{\boldsymbol{\Gamma}}$ into (10). Since $\mathbf{C} = \boldsymbol{\varphi}^*(\mathbf{g})$, one may show [57], using the properties of a linear connection (3.1) and the definition of the curvature tensor (3.9), that $\overset{\mathbf{C}}{\mathbf{R}} = \boldsymbol{\varphi}^*_{\mathbf{g}}(\overset{\mathbf{g}}{\mathbf{R}})$. Hence, if the tensor field $\overset{\mathbf{C}}{\mathbf{R}}$ is derivable from a motion function $\boldsymbol{\varphi}(\mathbf{X}, t)$ and if $\overset{\mathbf{C}}{\mathbf{R}} = \mathbf{0}$, then $\mathbf{C}$ is *compatible* and $\overset{\mathbf{C}}{\mathbf{R}} = \boldsymbol{\varphi}^*(\mathbf{0}) = \mathbf{0}$. Notice that $\mathbf{C}$-compatibility does not require specification of a unique current configuration, since $\mathbf{C}$ is independent of the rotation tensor $\mathbf{Q}$ associated with the right polar decomposition $\mathbf{F} = \mathbf{QU}$. Furthermore, as discussed by Truesdell and Noll [101] and Acharya and Bassani [100], even if $\mathbf{C}$ is compatible, the integrability of an arbitrary deformation gradient field $\mathbf{F}$ generating the strain field $\mathbf{C}$ may be destroyed by rotations $\mathbf{Q}$ that do not arise from rigid-body transformations of $\boldsymbol{\varphi}$. A material in such a condition is said to be in a state of *contorted aleotropy* in the sense of Noll [21]. The converse of the previous theorem has also been proven, albeit only locally [58]. In other words, given a positive-definite, symmetric, second-rank tensor $\mathbf{C}$ whose curvature vanishes (i.e. $\overset{\mathbf{C}}{\mathbf{R}} = \mathbf{0}$) then at any point with coordinates $X^A \in B_0$ there exists a neighborhood U_0 of X^A endowed with a mapping $\boldsymbol{\varphi}\colon B_0 \supset U_0 \to U \subset B$ whose deformation tensor is $\mathbf{C}$. One can consider $\mathbf{C}$-compatibility an outcome of deformation gradient compatibility ($\mathbf{F}$-compatibility), which is discussed next.

3.3. *Deformation gradient compatibility*

Consider now a field of contravariant (basis) vectors $\{\tilde{\mathbf{g}}_\alpha\}$, where $(\alpha = 1, 2, 3)$, spanning configuration space $\tilde{B}$. By introducing the two-point deformation map $\tilde{\mathbf{F}} = \tilde{F}^\alpha_{\ .A}\, \tilde{\mathbf{g}}_\alpha \otimes \mathbf{G}^A$, which we assume is defined globally, we can push forward vectors $\mathbf{V} \in TB_0$ to the tangent bundle $T\tilde{B}$:

$$\tilde{\mathbf{F}}\mathbf{V} = \tilde{F}^\alpha_{\ .A} \tilde{\mathbf{g}}_\alpha \otimes \mathbf{G}^A \left(V^B \mathbf{G}_B\right) = \tilde{F}^\alpha_{\ .A} V^B \tilde{\mathbf{g}}_\alpha \langle \mathbf{G}^A, \mathbf{G}_B \rangle = \tilde{F}^\alpha_{\ .A} V^B \delta^A_B \tilde{\mathbf{g}}_\alpha = \tilde{F}^\alpha_{\ .A} V^A \tilde{\mathbf{g}}_\alpha \in T\tilde{B}. \tag{14}$$

The basis vectors are tangent to globally-continuous coordinate curves $\tilde{x}^\alpha$ (i.e. $\tilde{\mathbf{g}}_\alpha = \partial_\alpha \tilde{\mathbf{x}}$ for some coordinate parameterization $\tilde{x}^\alpha(\mathbf{X})$) if and only if the following integrability conditions hold for $\tilde{\mathbf{F}}$ [55]:

$$\partial_B \tilde{F}^\alpha_{\ .A} = \partial_A \tilde{F}^\alpha_{\ .B} \leftrightarrow \frac{\partial^2 \tilde{x}^\alpha}{\partial X^A \partial X^B} = \frac{\partial^2 \tilde{x}^\alpha}{\partial X^B \partial X^A}. \tag{15}$$

If the conditions (15) are not satisfied, then $\{\tilde{\mathbf{g}}_\alpha\}$ is called an *anholonomic coordinate basis*, the deformation map $\tilde{\mathbf{F}}$ is called an *incompatible map*, and the configuration space $\tilde{\boldsymbol{B}}$ is called an *incompatible configuration* or an *anholonomic space*. Since conventional partial differentiation with respect to anholonomic coordinates does not apply, we define differentiation with respect to the $\tilde{x}^\alpha$ as

$$\frac{\partial(\cdot)}{\partial\tilde{x}^\alpha} \equiv \frac{\partial(\cdot)}{\partial X^A}\tilde{F}^{-1A}_{.\alpha} \leftrightarrow \partial_\alpha(\cdot) \equiv \partial_{\mathrm{A}}(\cdot)\tilde{F}^{-1A}_{.\alpha}. \tag{16}$$

A Levi–Civita connection (i.e. a connection both torsion-free and metric with respect to $\tilde{\mathbf{g}}$, the latter with components $\tilde{g}_{\alpha\beta} = \tilde{\mathbf{g}}_\alpha \cdot \tilde{\mathbf{g}}_\beta$) on $\tilde{\boldsymbol{B}}$ may not exist, since the field of tangent vectors $\{\tilde{\mathbf{g}}_\alpha\}$ may not be sufficiently smooth over all of $\tilde{\boldsymbol{B}}$ to admit coordinate differentiation (with respect to coordinates that may in fact not exist, i.e. anholonomic coordinates). However, in the anholonomic (intermediate or natural) configurations of elastoplasticity theory, each local volume element is often referred to an external system of coordinates with Euclidean metric tensor, typically taken as a global Cartesian frame [64, 65], although such an assumption is not necessary from a physical perspective [2, 66]. The Riemann–Christoffel curvature formed from the covariant strain measure $\tilde{C}_{AB} \equiv \tilde{F}^\alpha_{.A}\tilde{g}_{\alpha\beta}\tilde{F}^\beta_{.B}$ does not necessarily vanish (unless holonomic $\tilde{x}^\alpha$ are available), in contrast to the curvature tensor derived from connection (13) formed from the deformation $\mathbf{C}$.

4. Deformation gradient kinematics

Our framework encompasses kinematic descriptions at two length scales, which we shall refer to henceforth as the macroscale and the microscale. The macroscopic description, predicated upon the multiplicative decomposition of the deformation gradient, describes the elastic–plastic kinematics for a volume element of crystalline material in an average sense. The microscopic description, predicated upon an additively-decomposed linear connection, embodies higher spatial gradients of lattice deformation as discussed in section 5, enabling one to interpolate for lattice stretch and orientation between centroids of neighboring elements.

Let $\mathbf{F}$ denote the volume-averaged deformation gradient (equation (11)) for an element of crystalline material. Most generally, we decompose $\mathbf{F}$ multiplicatively as

$$\mathbf{F} \equiv T\boldsymbol{\varphi} = \frac{\partial\mathbf{x}}{\partial\mathbf{X}} = \mathbf{F}^{\boldsymbol{L}}\mathbf{F}^{\mathbf{p}} = \mathbf{F}^{\mathbf{e}}\mathbf{F}^{\mathbf{i}}\mathbf{F}^{\mathbf{p}}, \tag{17}$$

where $\mathbf{F}^{\boldsymbol{L}} \equiv \mathbf{F}^{\mathbf{e}}\mathbf{F}^{\mathbf{i}}$ represents the total lattice deformation, $\mathbf{F}^{\mathbf{e}}$ is the recoverable elastic deformation, and $\mathbf{F}^{\mathbf{p}}$ is the plastic deformation, leaving $\mathbf{F}^{\mathbf{i}}$ as the residual lattice deformation associated with defects and other sources of heterogeneity. None of the mappings $\mathbf{F}^{\mathbf{e}}$, $\mathbf{F}^{\mathbf{i}}$, $\mathbf{F}^{\mathbf{p}}$, or $\mathbf{F}^{\boldsymbol{L}}$ need be holonomic when considered from the scale of neighboring volume elements. The inverse of the recoverable elastic deformation, $\mathbf{F}^{\mathbf{e}-1}$, is achieved via instantaneous traction removal from the surface of the crystalline element, and may include rigid body rotation of the solid as well as recoverable thermal deformation (e.g., average contraction of the lattice upon cooling to a reference temperature). Since lattice defects are not introduced during this hypothetical unloading process, $\mathbf{F}^{\mathbf{e}}$ does not alter the holonomicity (or lack thereof)

of the material *within* the volume element. However, since the deformation achieved upon unloading may not be compatible across neighboring elements, $\mathbf{F}^{\mathbf{e}}$ is anholonomic at the macroscale. The deformation $\mathbf{F}^{\mathbf{p}}$ embodies contributions of defects that leave the lattice unperturbed in an average sense, e.g. dislocation glide. Finally, $\mathbf{F}^{\mathbf{i}}$ accounts for remaining physics, including

- Residual strain and rotation fields attributed to non-redundant (i.e. geometrically necessary) dislocations [67]
- Rotation of the lattice attributed to rotational defects (i.e. disclinations), which may describe subgranular defect walls formed during large deformations (*cf*. [68]) or deformation twins [69, 70]
- Residual thermal strains due to heterogeneous thermal expansion properties within the volume element, perhaps induced by defects in the microstructure
- Volumetric defects such as interstitials or voids resulting in lattice expansion or contraction
- Phase transformations that alter the lattice arrangement [70]

Decomposition (17) and the $\mathbf{F}^{\mathbf{i}}$ deformation mapping were introduced by the present authors to describe elastoplastic polycrystals [71] and elastoplastic single crystals [67], both in the context of dislocation-based crystal plasticity theory. The concept is generalized here to account for various residual lattice deformation modes listed above. Note that (17) is scale dependent, depending upon the size of the crystal volume element to which it is applied, and resolution dependent, depending upon the way in which local kinematics within the volume element are resolved and accounted for in the description. For example, the relative magnitudes of components of $\mathbf{F}^{\mathbf{i}}$ will differ for a single crystal containing a few non-redundant dislocations and a heterogeneously-deforming polycrystal supporting large residual stresses due to intergranular incompatibility. Kratochvíl [72] postulated a three-term decomposition similar to (17), although the length scale dependence was not emphasized. Our theory reduces to one suggested by Bilby and Smith [99] for residual elastoplasticity when $\mathbf{F}^{\mathbf{e}} = \mathbf{1}$ and the elastic unloading corresponds to global unloading, leading to the reduced decomposition $\mathbf{F} = \mathbf{F}^{\mathbf{i}}\mathbf{F}^{\mathbf{p}}$ (see [73]). And our decomposition reduces to that of Lardner [44, 74] and Peçherski [51, 52] when we set $\mathbf{F}^{\mathbf{i}} = \tilde{\mathbf{R}}$, where $\tilde{\mathbf{R}}$ is an orthogonal matrix describing lattice rotation caused by disclinations.

Macroscopic configurations of a crystalline element corresponding to (17) are depicted in figure 1. Intermediate configurations $\bar{B}$ and $\tilde{B}$ are generally anholonomic, spanned by anholonomic coordinates $\bar{x}^{\bar{\alpha}}$ and $\tilde{x}^{\alpha}$, respectively, while reference and spatial configurations B_0 and B are holonomic, spanned by continuous coordinates X^A and x^a, respectively. Configuration B supports nonzero traction vector $\mathbf{t}$, while configurations $\bar{B}$ and $\tilde{B}$ are traction free, i.e. $\mathbf{t} = \mathbf{0}$ and $\tilde{\mathbf{t}} = \mathbf{0}$. Lattice director vectors are mapped across configurations via

$$\mathbf{d}_a = \left(F^{L-1}\right)_{.a}^{\bar{\alpha}} \mathbf{d}_{\bar{\alpha}}, \quad \mathbf{d}_{\alpha} = \left(F^{i-1}\right)_{.\alpha}^{\tilde{\alpha}} \mathbf{d}_{\tilde{\alpha}}, \quad \mathbf{d}_a = \left(F^{e-1}\right)_{.a}^{\alpha} \mathbf{d}_{\alpha}, \tag{18}$$

while $\mathbf{F}^{\mathbf{p}}$ is assumed to leave the lattice unperturbed. When the lattice directors are heterogeneous within the crystalline volume element (e.g. in polycrystals or in subdivided single crystals), the triads of (18) and figure 1 are understood to

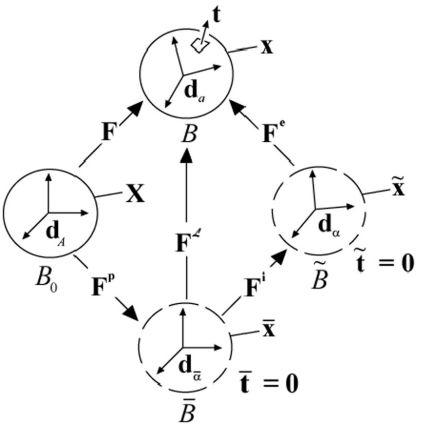

Figure 1. Deformation mappings and configurations for crystalline volume element.

represent suitably-defined 'average' directors for the volume element [75]. In non-cubic lattices, the directors of (18) are not necessarily parallel to primitive translation vectors of the unit cell, but are instead an external construct. Upon assuming that the directors in $\bar{B}$ are orthonormal, and assigning an external Cartesian coordinate system to anholonomic space $\bar{B}$ with metric tensor

$$\mathbf{d}_{\bar{\alpha}} \cdot \mathbf{d}_{\bar{\beta}} = \bar{g}_{\bar{\alpha}\bar{\beta}} = \delta_{\bar{\alpha}\bar{\beta}}, \tag{19}$$

we define a metric tensor $\mathbf{C}^L$ referred to configuration B and associated with the director strain:

$$C^L_{ab} \equiv \mathbf{d}_a \cdot \mathbf{d}_b = F^{L-1\bar{\alpha}}_{.a} F^{L-1\bar{\beta}}_{.b} \mathbf{d}_{\bar{\alpha}} \cdot \mathbf{d}_{\bar{\beta}} = F^{L-1\bar{\alpha}}_{.a} \delta_{\bar{\alpha}\bar{\beta}} F^{L-1\bar{\beta}}_{.b}. \tag{20}$$

The metric $\mathbf{C}^L$ will play a prominent role in the continuation of our framework in section 5.

The particular sequence of deformation maps in (17) is chosen based on rational arguments. The plastic deformation term $\mathbf{F^p}$ is the rightmost in our decomposition, as it leaves the lattice vectors unaltered, permitting identification of configuration $\bar{b}$ of figure 1 with Mandel's [76] isoclinic configuration. The residual deformation due to micro-heterogeneity in the presence of lattice defects, $\mathbf{F^i}$, is placed second, as it affects the lattice directors via (18), yet is assumed unaffected by superposed rigid body motion or a change in spatial coordinate frame [72]. Finally, the recoverable elastic deformation $\mathbf{F^e} = \mathbf{V^e R^e}$ logically assumes the leftmost position, as the stretch $\mathbf{V^e}$ is associated with unloading of the average traction acting on the volume element from the *current* state and the orthogonal matrix $\mathbf{R^e}$ accounts for all lattice rotations not embodied in $\mathbf{F^i}$, including net rigid body motions of the solid. The rotational components $\mathbf{R^i}$ of $\mathbf{F^i}$ and $\mathbf{R^p}$ of $\mathbf{F^p}$ are assumed to evolve independently of rigid body motions of the solid. Although numerous decompositions are possible (*cf.* [77]), we find our description (17) most appropriate and realistic from the physical standpoint.

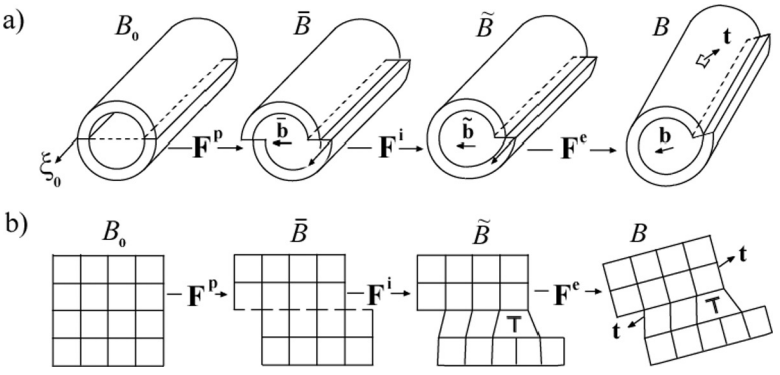

Figure 2. Configurations of crystal element containing edge dislocation: (a) Volterra model and (b) lattice model.

Figure 2 describes the physics of equation (17) from the standpoint of (a) a Volterra process and (b) a cubic crystalline lattice for a volume element containing a single edge dislocation. The tangent line of the defect is written as $\boldsymbol{\xi}_0$, and the Burgers vector is labeled $\mathbf{b}$, with adornments corresponding to the particular configuration. Notice how the displacement discontinuity in the wake of the dislocation is sealed by the residual lattice deformation $\mathbf{F}^{\mathbf{i}}$. Prior to the application of $\mathbf{F}^{\mathbf{i}}$, for the body labeled $\bar{\boldsymbol{B}}$ in figure 2, elastic strain fields are absent, and the plastic deformation gradient $\mathbf{F}^{\mathbf{p}}$ is completely defined in terms of the relative motion of the two halves of the lattice on opposite sides of the slip plane (dotted line in figure (2b)). Note also that $\bar{\boldsymbol{B}}$ is generally locally incompatible across the entire slip path, contains slip discontinuities but no lattice strains, and is free of internal residual stress fields. This is in contrast to $\tilde{\boldsymbol{B}}$, which may contain internal residual stress and lattice strain fields but includes no discontinuities except for those in the immediate vicinity of individual defect lines contained within the volume.

5. Micromorphic kinematics

At the microscopic level, spatial changes in the lattice directors $\mathbf{d}_a$ are described by parallel transport with respect to a linear connection. The absolute change of the director vector field in the current configuration is found in terms of the covariant derivative $\hat{\nabla}$, i.e.

$$\hat{\nabla}_b \mathbf{d}_a = \mathbf{d}_{a,b} - \hat{\Gamma}^{\cdot\cdot c}_{ba} \mathbf{d}_c, \tag{21}$$

with the subscripted comma denoting partial coordinate differentiation with respect to $\mathbf{x}$. The Christoffel symbols of the connection are defined by [45, 46]

$$\hat{\Gamma}^{\cdot\cdot a}_{cb} \equiv F^{La}_{\cdot\bar{\alpha}} F^{L-1\bar{\alpha}}_{\cdot b,c} + Q^{\cdot\cdot a}_{cb} = \bar{\Gamma}^{\cdot\cdot a}_{cb} + Q^{\cdot\cdot a}_{cb}, \tag{22}$$

where $\bar{\Gamma}^{\cdot\cdot a}_{cb} \equiv F^{La}_{\cdot\bar{\alpha}} F^{L-1\bar{\alpha}}_{\cdot b,c} = -F^{La}_{\cdot\bar{\alpha},c} F^{L-1\bar{\alpha}}_{\cdot b}$ are coefficients of the crystal connection of non-Riemannian dislocation theories [4, 5, 19, 21], and $Q^{\cdot\cdot a}_{cb}$ are micromorphic degrees-of-freedom representing contributions of distributed defects to the spatial gradients of the lattice director field. Upon assuming that $\hat{\nabla}_b \mathbf{d}_a = 0$ [46], the connection (22) allows one to interpolate for the directions and magnitudes of the lattice directors between centroids of neighboring crystal volume elements. For example, in the trivial situation when $\hat{\Gamma}^{\cdot\cdot a}_{cb} = 0$, the lattice directors are spatially constant. The crystal connection ($\bar{\boldsymbol{\Gamma}}$) component of (22) accounts for effects of first-order spatial gradients of (the inverse of) $\mathbf{F}^L$, while the micromorphic variable $\mathbf{Q}$ of (22) accounts for additional spatial variations of lattice directors not captured by the first gradient of $\mathbf{F}^L$. The average continuum deformation of the director vectors located at the volume element's centroid is determined by $\mathbf{F}^L$, as indicated by equation (18). Lattice stretch and rotation gradients (e.g. at the scale of subgrain cells and cell blocks (*cf.* [68, 78]) are represented by the coefficients of equation (22).

The covariant components of $\mathbf{Q}$ are defined via lowering by the metric $\mathbf{C}^L$ of equation (20):

$$Q_{cba} \equiv Q^{\cdot\cdot d}_{cb} C^L_{da}. \tag{23}$$

Quantities Q_{cba} and $Q^{\cdot\cdot a}_{cb}$ are effectively equivalent micro-deformation measures only when lattice strains are negligible, i.e. when $C^L_{da} \approx \delta_{da}$. The covariant derivative of $\mathbf{C}^L$ is found as

$$\hat{\nabla}_c C^L_{ab} = \underbrace{C^L_{ab,c} - \bar{\Gamma}^{\cdot\cdot d}_{ca} C^L_{db} - \bar{\Gamma}^{\cdot\cdot d}_{cb} C^L_{ad}}_{=0} - Q^{\cdot\cdot d}_{ca} C^L_{db} - Q^{\cdot\cdot d}_{cb} C^L_{ad} = -2Q_{c(ab)}, \tag{24}$$

where parentheses denote symmetrization, e.g. $2Q_{c(ba)} = Q_{cba} + Q_{cab}$. Components of the torsion tensor $\hat{\mathbf{T}}$ of the connection $\hat{\boldsymbol{\Gamma}}$ are given by (see equation (7))

$$\hat{T}^{\cdot\cdot a}_{cb} \equiv \hat{\Gamma}^{\cdot\cdot a}_{cb} - \hat{\Gamma}^{\cdot\cdot a}_{bc} = \bar{T}^{\cdot\cdot a}_{cb} + 2Q^{\cdot\cdot a}_{[cb]}, \tag{25}$$

where $\bar{T}^{\cdot\cdot a}_{cb}$ is the torsion of the crystal connection. The components of the Riemann–Christoffel curvature tensor $\hat{R}^{\cdot\cdot\cdot a}_{bcd}$ formed from the connection coefficients $\hat{\Gamma}^{\cdot\cdot a}_{cb}$ are found using equation (10):

$$\hat{R}^{\cdot\cdot\cdot a}_{bcd} \equiv \hat{\Gamma}^{\cdot\cdot a}_{db,c} - \hat{\Gamma}^{\cdot\cdot a}_{cb,d} + \hat{\Gamma}^{\cdot\cdot a}_{ce} \hat{\Gamma}^{\cdot\cdot e}_{db} - \hat{\Gamma}^{\cdot\cdot a}_{de} \hat{\Gamma}^{\cdot\cdot e}_{cb}, \tag{26}$$

which, because $\hat{\Gamma}^{\cdot\cdot a}_{cb} = \bar{\Gamma}^{\cdot\cdot a}_{cb} + Q^{\cdot\cdot a}_{cb}$, we are able to rewrite as [55]

$$\hat{R}^{\cdot\cdot\cdot a}_{bcd} = \underbrace{\bar{R}^{\cdot\cdot\cdot a}_{bcd}}_{=0} + 2\hat{\nabla}_{[c} Q^{\cdot\cdot a}_{d]b} + Q^{\cdot\cdot a}_{ce} Q^{\cdot\cdot e}_{db} - Q^{\cdot\cdot a}_{de} Q^{\cdot\cdot e}_{cb} + \hat{T}^{\cdot\cdot e}_{cd} Q^{\cdot\cdot a}_{eb}, \tag{27}$$

where the curvature from the crystal connection, $\bar{R}^{\cdot\cdot\cdot a}_{bcd}$, vanishes identically as shown, since $\bar{\boldsymbol{\Gamma}}$ is integrable (see equation (53)). The fully covariant curvature $\hat{R}_{abcd} \equiv C^L_{af} \hat{R}^{\cdot\cdot\cdot f}_{bcd}$ is [45]

$$\hat{R}_{[ab]cd} = 2\hat{\nabla}_{[c} Q_{d][ba]} + \hat{T}^{\cdot\cdot e}_{cd} Q_{e[ba]}, \quad \hat{R}_{(ab)cd} = 2\hat{\nabla}_{[c} Q_{d](ab)} + \hat{T}^{\cdot\cdot e}_{cd} Q_{e(ab)}. \tag{28}$$

We see from (28) that $\hat{\mathbf{R}}$ vanishes completely when $\mathbf{Q} = \mathbf{0}$.

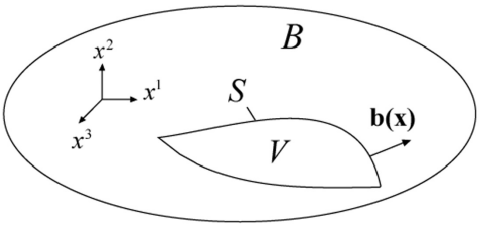

Figure 3. Somigliana dislocation.

The concept of a Somigliana dislocation [79] can be used to characterize the displacement discontinuities from translational and rotational dislocations (i.e. disclinations) of Volterra [41], point defects [10, 11] and interface incompatibility in multi-phase composites [49]. A Somigliana dislocation may be idealized in terms of a closed volume V bounded by surface S located within the interior of a body B of infinite size, as shown in figure 3. The surface S is first cut, and the two faces of the cut undergo a small relative displacement $\mathbf{b}(\mathbf{x})$, where $\mathbf{x}$ is the position of the point on the surface S. When $\mathbf{b}(\mathbf{x})$ produces separation of matter, the empty space is then filled. On the other hand, when $\mathbf{b}(\mathbf{x})$ produces an overlap of material, we consider the extra material to be subsequently removed. The faces of S are cemented together, such that any further displacements are continuous across S. The body containing the Somigliana defect is now in a state of internal stress (see also [50]).

If $\mathbf{b}(\mathbf{x}) = \textit{constant}$, the Somigliana dislocation is equivalent to the usual translational dislocation of Volterra [41] and Burgers [80]. If $\mathbf{b}(\mathbf{x}) = \boldsymbol{\omega} \times \mathbf{r}(\mathbf{x})$, where $\boldsymbol{\omega}$ is the spatially constant Frank vector [81] and $\mathbf{r}$ is the disclination radius, the Somigliana defect is equivalent to the disclination of Volterra [41] and Frank [81]. To model a point defect, we let S be a small sphere with a distribution of $\mathbf{b}(\mathbf{x})$ over the surface. Letting the radius of S shrink to zero, while at the same time prescribing $\mathbf{b}(\mathbf{x})$ such that the displacement at a fixed distance from the sphere remains finite, provides a mechanical representation of a point singularity [11]. For the particular case of $\mathbf{b}(\mathbf{x})$ constant and directed radially outward from S, we obtain a model of a spherical interstitial or substitutional atom, while a vacancy is modeled for $\mathbf{b}(\mathbf{x})$ directed inward. By considering a uniform distribution of somewhat larger hollow spheres, we can model porosity associated with microvoids in crystals.

We now make the association of the general micromorphic framework of (21)–(28) with the physics of crystal defects. This is accomplished by considering three limiting cases: traditional (geometrically-necessary) dislocation theory, characterized by $Q_{cba} = 0$; disclination theory, characterized by $Q_{cba} = Q_{c[ba]}$; and a model for isotropically-distributed point defects, characterized by $Q_{cba} = Q_c C^L_{ba}$. Superposition of the three cases then enables us to consider Somigliana dislocations of arbitrary character.

5.1. *Dislocations*

The description afforded by our framework is restricted to translational dislocations if we prescribe $Q_{cba} = 0$, for which (22) reduces to the crystal connection [19]:

$$\hat{\Gamma}^{..a}_{cb} = \bar{\Gamma}^{..a}_{cb} = F^{La}_{.\bar{\alpha}} F^{L-1\bar{\alpha}}_{.b,\,c} = -F^{La}_{.\bar{\alpha},\,c} F^{L-1\bar{\alpha}}_{.b}. \tag{29}$$

The torsion tensor of (29) is then written as

$$\hat{T}^{..a}_{cb} = \bar{T}^{..a}_{cb} = F^{La}_{.\bar{\alpha}} F^{L-1\bar{\alpha}}_{.[b,\,c]}, \tag{30}$$

which vanishes according to (35) when the lattice deformation is holonomic, i.e.

$$\bar{T}^{..a}_{cb} = 0 \leftrightarrow F^{L-1\bar{\alpha}}_{.[b,\,c]} = 0 \leftrightarrow F^{L-1\bar{\alpha}}_{.a} = \partial_a \bar{x}^{\bar{\alpha}}. \tag{31}$$

Figure 4 provides a two-dimensional visual interpretation. On the left side of figure 4, we inscribe two orthogonal fields of constant contravariant 'lattice slip vectors' on $\bar{B}$ — denoted by $\mathbf{u}$ and $\mathbf{v}$ — that form a rectilinear grid. Such a representation of a 'perfect' lattice in $\bar{B}$ is in agreement with classical crystal plasticity theory [82], for example, wherein $\mathbf{F^p}$ is assumed to leave the slip directions unperturbed. Notice that the lattice may have slipped with respect to its position relative to the reference configuration B_0, consistent with figure 2(b) and indicated by the dotted unit cells on the left side of figure 4 (for clarity, these slip steps are not shown on the right side of figure 4, though they do exist in configuration B). Since the lattice slip vectors are spatially constant over the relaxed crystal, we have

$$\mathbf{u}(A) = \mathbf{u}(B), \quad \mathbf{v}(A) = \mathbf{v}(B), \tag{32}$$

where A and B are two neighboring points in the relaxed configuration that are separated by a small distance $d\mathbf{x} \equiv \mathbf{x}(A) - \mathbf{x}(B)$ when mapped onto the deformed coordinates of the crystal. Focusing for the moment on the field $\bar{\mathbf{u}}$, we multiply both sides of the first of (32) by $\mathbf{F}^L(A)$, the value of the lattice deformation at the location corresponding to point A, to obtain

$$F^{La}_{.\bar{\alpha}}(A)\bar{u}^{\bar{\alpha}}(A) = F^{La}_{.\bar{\alpha}}(A)\bar{u}^{\bar{\alpha}}(B). \tag{33}$$

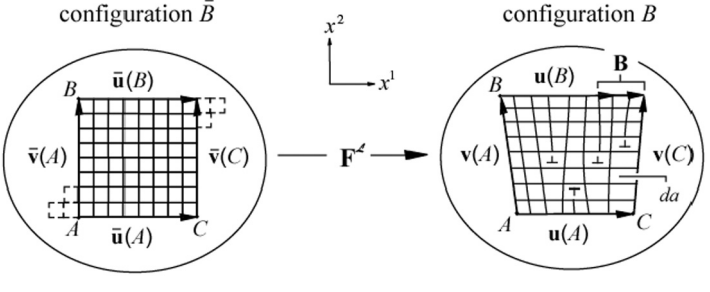

Figure 4. Visualization of the crystal connection.

Expanding $\mathbf{F}^L(A)$ with a first-order (i.e. linear) approximation in $\mathbf{x}$, we have

$$F^{La}_{.\bar{\alpha}}(A) \approx F^{La}_{.\bar{\alpha}}(B) + F^{La}_{.\bar{\alpha},b}(B)dx^b, \tag{34}$$

which is then substituted into equation (33) to yield

$$u^a(A) = u^a(B) + F^{La}_{.\bar{\alpha},b}(B)F^{L-1\bar{\alpha}}_{.c}(B)dx^b u^c(B), \tag{35}$$

where we have defined the deformed slip vectors as push-forwards via

$$u^a(A) \equiv F^{La}_{.\bar{\alpha}}(A)\bar{u}^{\bar{\alpha}}(A), \quad u^a(B) \equiv F^{La}_{.\bar{\alpha}}(B)\bar{u}^{\bar{\alpha}}(B). \tag{36}$$

Using the identity $(F^{La}_{.\bar{\alpha}}F^{L-1\bar{\alpha}}_{.c})_{,b} = 0$, we can rewrite equation (35) as

$$0 = u^a(A) - u^a(B) + F^{La}_{.\bar{\alpha}}(B)F^{L-1\bar{\alpha}}_{.c,b}(B)dx^b u^c(B). \tag{37}$$

Making the linear approximation

$$u^a(A) - u^a(B) \approx \frac{\partial u^a(B)}{\partial x^b}\underbrace{\left(x^b(A) - x^b(B)\right)}_{\equiv dx^b}, \tag{38}$$

and dropping the notation signaling localization to point B, equation (37) then becomes

$$0 = u^a_{.,b}dx^b + F^{La}_{.\bar{\alpha}}F^{L-1\bar{\alpha}}_{.c,b}dx^b u^c, \tag{39}$$

which obtains the structure of a null covariant derivative, i.e. parallel transport:

$$\bar{\nabla}_b u^a \equiv u^a_{.,b} + \bar{\Gamma}^{.a}_{bc}u^c = 0, \tag{40}$$

since dx^b is now arbitrary. Since the Christoffel symbols corresponding to $\bar{\nabla}$ in (40) are equivalent to those given in equation (29), parallel transport of the slip vectors with respect to the crystal connection physically corresponds to construction of the deformed lattice from a rectilinear grid in relaxed configuration $\bar{\boldsymbol{B}}$. Analogously, the field $\mathbf{v}$ in figure 4 satisfies

$$\bar{\nabla}_b v^a \equiv v^a_{.,b} + \bar{\Gamma}^{.a}_{bc}v^c = 0, \tag{41}$$

i.e. the vector field $\mathbf{v} = \mathbf{F}^L\mathbf{v} \in TB$ constructed by pushing forward from the uniform reference grid $\mathbf{v} \in T\bar{\boldsymbol{B}}$ obeys the rule of parallel transport with respect to the connection $\bar{\boldsymbol{\Gamma}}$. It is clear why the crystal connection is said to possess the property of 'distant parallelism' or 'teleparallelism'.

The closure failure $\mathbf{B}$ of the area a (with local differential one-form $n_c da = \varepsilon_{cab}dx^a \wedge dx^b$, where n_c denotes a unit vector normal to a) shown in figure 4—i.e. the area of the parallelogram enclosed by $\mathbf{u}(A), \mathbf{u}(B), \mathbf{v}(A)$, and $\mathbf{v}(C)$, with C a third location on the deformed crystal—is equivalent to the area integral

of the field of local Burgers vectors $\mathbf{b}(\mathbf{x})$ [53]:

$$B^a \equiv \int_a b^a \, da = \int_a \alpha^{ab} n_b \, da = \frac{1}{2} \int_a \bar{T}^{\cdot a}_{bc} dx^b \wedge dx^c, \tag{42}$$

where $2\alpha^{ab} \equiv \varepsilon^{bdc} \bar{T}^{\cdot a}_{dc}$ is the geometrically necessary dislocation density tensor referred to B. In terms of straight defect lines, the dislocation density tensor is written [30, 74]

$$\boldsymbol{\alpha} = \sum_j \rho^j \mathbf{b}^j \otimes \boldsymbol{\xi}^j, \tag{43}$$

with ρ^j, $\mathbf{b}^j$, and $\boldsymbol{\xi}^j$ the line length per unit current volume, Burgers vector, and tangent line in the spatial configuration for dislocation population j. To deduce (42) directly from the right side of figure 4, we begin with the rather obvious vector addition relation

$$B^a = u^a(A) - u^a(B) + v^a(C) - v^a(A). \tag{44}$$

Also from the current configuration lattice depicted in figure 4 we have

$$\overset{(u)}{dx^b} \equiv x^b(B) - x^b(A) = v^b(A), \quad \overset{(v)}{dx^b} \equiv x^b(C) - x^b(A) = u^b(A). \tag{45}$$

Upon making the linear approximations

$$u^a(B) - u^a(A) \approx u^a_{,b}(A) \overset{(u)}{dx^b}, \quad v^a(C) - v^a(A) \approx v^a_{,b}(A) \overset{(v)}{dx^b}, \tag{46}$$

and invoking equations (40) and (41), equation (44) becomes

$$B^a = -u^a_{,b}(A) \overset{(u)}{dx^b} + v^a_{,b}(A) \overset{(v)}{dx^b} = \bar{\Gamma}^{\cdot a}_{bc} \overset{(u)}{dx^b} u^c(A) - \bar{\Gamma}^{\cdot a}_{bc} \overset{(v)}{dx^b} v^c(A), \tag{47}$$

which upon usage of (45) can be written as

$$B^a = 2\bar{\Gamma}^{\cdot a}_{[bc]} v^b(A) u^c(A) = \bar{T}^{\cdot a}_{bc} (v(A)u(A))^{[bc]}. \tag{48}$$

Making the identification

$$(v(A)u(A))^{[bc]} = \frac{1}{2}\left(v^b(A)u^c(A) - v^c(A)u^b(A)\right) \equiv \frac{1}{2} dx^b \wedge dx^c, \tag{49}$$

equation (48) is then rewritten as

$$B^a = \frac{1}{2} \bar{T}^{\cdot a}_{bc} dx^b \wedge dx^c, \tag{50}$$

which is the local form of (42). Integrability conditions for the crystal connection coefficients of equation (29) have a natural geometric interpretation, as demonstrated in previous works by Schouten [55] and Le and Stumpf [4]. Partial coordinate differentiation of (29) yields

$$\left(F^{L-1\bar{\alpha}}_{\cdot a} \bar{\Gamma}^{\cdot a}_{bc}\right)_{,d} = F^{L-1\bar{\alpha}}_{\cdot c,bd}, \tag{51}$$

the left side of which is expanded to read

$$F^{L-1\bar{\alpha}}_{.a,d}\bar{\Gamma}^{..a}_{bc} + F^{L-1\bar{\alpha}}_{.a}\bar{\Gamma}^{..a}_{bc,d} = F^{L-1\bar{\alpha}}_{.a}\left(\bar{\Gamma}^{..a}_{de}\bar{\Gamma}^{..e}_{bc} + \bar{\Gamma}^{..a}_{bc,d}\right). \tag{52}$$

Since the order of partial differentiation on the right side of (51) is arbitrary, we then have

$$0 = -2F^{L-1\bar{\alpha}}_{.c,[bd]} = F^{L-1\bar{\alpha}}_{.a}\left(\bar{\Gamma}^{..a}_{dc,b} - \bar{\Gamma}^{..a}_{bc,d} + \bar{\Gamma}^{..a}_{be}\bar{\Gamma}^{..e}_{dc} - \bar{\Gamma}^{..a}_{de}\bar{\Gamma}^{..e}_{bc}\right) = F^{L-1\bar{\alpha}}_{.a}\bar{R}^{...a}_{cbd}, \tag{53}$$

where $\bar{R}^{...a}_{cbd}$ are the components of the Riemann–Christoffel curvature tensor derived from $\bar{\Gamma}^{..a}_{bc}$ using (10). Upon multiplication of (53) through by $\mathbf{F}^L$ we arrive at the conclusion that $\bar{R}^{...a}_{cbd} = 0$ are conditions ensuring satisfaction of (29). From satisfaction of (53), the crystal connection is said to be 'integrable' [55]. Since the crystal connection is metric with respect to $\mathbf{C}^L$ (from equation (24) with $Q^{..a}_{bc} = 0$), and its curvature tensor vanishes, the set $\{B, \bar{\boldsymbol{\Gamma}}, \mathbf{C}^L\}$ constitutes a *metric, non-Riemannian space*. We also have

$$2C^L_{ab}\bar{\Gamma}^{..a}_{(cd)} = C^L_{cb,d} + C^L_{db,c} - C^L_{dc,b}, \tag{54}$$

easily verified by direct calculation. If we now further impose that the torsion $\bar{T}^{..a}_{cb} = 0$, such that $\bar{\Gamma}^{..a}_{cb} = \bar{\Gamma}^{..a}_{(cb)}$, meaning that the connection is symmetric (i.e. non-Cartan space), and physically that geometrically necessary dislocations are absent, then (54) defines the *Levi–Civita connection coefficients* (*cf.* (8)) on the current configuration with Riemannian metric tensor $\mathbf{C}^L$, and the set $\{B, \bar{\boldsymbol{\Gamma}}, \mathbf{C}^L\}$ constitutes a *Euclidean space*.

5.2. *Disclinations*

Volterra [41] introduced six fundamental types of defects in elastic bodies: three types of translational displacement discontinuities, known as edge and screw dislocations, and three types of rotational incompatibilities, later termed disclinations by Frank [81] and further classified as either wedge or twist disclinations (see figure 5). Disclination theory has been applied to numerous problems of interest. These include descriptions of micropolar rotations in liquid crystals [81], rotational defect substructures and commensurate strain hardening in metal forming processes [83], grain boundary structures [84], deformation twins [69], and polycrystalline triple junctions [85]. Disclinations have also been recognized as characteristic defects in polymers [86] and nanocrystals [87]. Molecular dynamics simulations incorporating disclination concepts [88, 89] have been undertaken to characterize energy distributions over a range of misorientations.

Continuum theories of distributed dislocations and disclinations can be found in the geometrically-oriented papers of Anthony [43], Eringen and Claus [73], Lardner [44], Minagawa [45, 46], Amari [47] and De Wit [48]. Precise mathematical descriptions and/or elastic solutions are also included in the texts of Nabarro [42], Lardner [74], Mura [90], Maugin [1] and Zubov [91]. An extensive review of disclination theory focusing upon defect kinetics and contributions to plastic strain hardening was provided by Seefeldt [78], who suggested that partial disclination dipoles be used to describe misoriented subgranular interfaces manifesting upon grain refinement

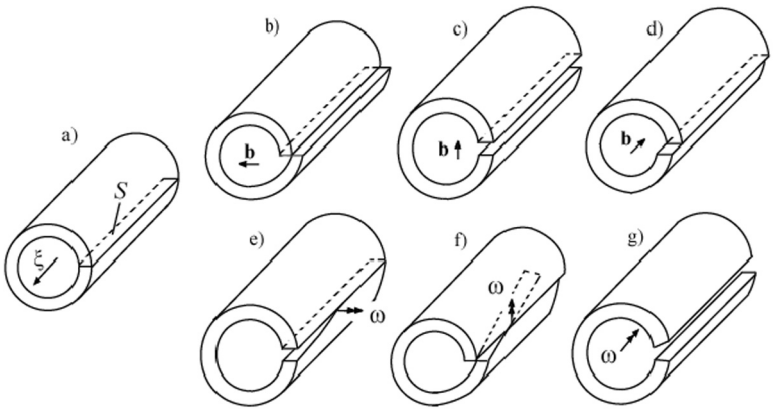

Figure 5. Volterra's defects: reference cylinder with defect line $\boldsymbol{\xi}$ and cut surface S (a); edge dislocations (b, c) and screw dislocation (d) with Burgers vector **b**; twist disclinations (e, f) and wedge disclination (g) with Frank vector $\boldsymbol{\omega}$.

in advanced stages of plastic deformation. Li [84, 92] demonstrated for a volume of isotropic linear-elastic solid material the equivalence between the strain energy of a wedge disclination dipole and a finite wall of edge dislocations. Kröner and Lagoudas [93] developed a gauge theory of disclinations intended to model micro-rotations in liquid crystals. Lazar and Maugin [94] solved for the stress field of a wedge disclination using higher gradient elasticity theory.

The coefficients $\hat{\Gamma}^{\cdot\cdot a}_{cb}$ in the dislocation-disclination version of our framework are given by equation (22), with the covariant components of **Q** anti-symmetric [45, 46]:

$$Q_{cba} \equiv Q^{\cdot\cdot d}_{cb} C^{L}_{da} = -Q_{cab} = Q_{c[ba]}. \tag{55}$$

The micro-rotation kinematic variable **Q** describes spatial gradients of lattice rotation within the crystalline volume element arising from distributed disclinations. Consider parallel transport of a lattice director $\mathbf{d}_a$, over the small distance $d\mathbf{x}$ to a new orientation $\mathbf{d}'_a$, conducted with respect to the covariant derivative (21). For illustrative purposes, we temporarily restrict attention the special case when $\mathbf{F}^L \approx \mathbf{1}$ and spatial gradients of the lattice deformation $\mathbf{F}^L$ are small. Applying the summation convention over covariant Cartesian coordinates, we may then write

$$\mathbf{d}'_a = \mathbf{d}_a + \mathbf{d}_{a,b} dx_b = \mathbf{d}_a + Q_{bac} dx_b \mathbf{d}_c = \big(\delta_{ac} + Q_{b[ac]} dx_b\big)\mathbf{d}_c = \Phi_{ac}\mathbf{d}_c, \tag{56}$$

where $Q_{bac} = Q_{b[ac]}$ from equation (55), and the rotation matrix Φ_{ac} satisfies $\mathbf{\Phi}^T \approx \mathbf{\Phi}^{-1}$ and $\det(\mathbf{\Phi}) \approx 1$ for small magnitudes of $Q_{bac} dx_b$, i.e. small relative lattice rotations such as those occurring across low-angle grain or subgrain boundaries. We see from (56) that Q_{bac} acts as an effective 'gradient' of rotation in the spatial direction x^b. However, since **Q** is *not* required to satisfy the following compatibility conditions, it is not a true spatial gradient, i.e.

$$Q_{b[ac],d} - Q_{d[ac],b} \neq 0 \rightarrow Q_{b[ac]} \neq \vartheta_{[ac],b}, \tag{57}$$

where $\vartheta_{[ac]}$ is a skew matrix that can exist only when the conditions $Q_{b[ac],d} = Q_{d[ac],b}$ are met.

We now return to the general situation wherein components of $\mathbf{F}^L$ may be arbitrarily large. From (24), the connection is metric, since the covariant derivative of $\mathbf{C}^L$ vanishes:

$$\hat{\nabla}_c C^L_{ab} = -2Q_{c(ab)} = 0. \tag{58}$$

Components of the torsion tensor $\hat{\mathbf{T}}$ of the connection $\hat{\mathbf{\Gamma}}$ are given by

$$\hat{T}^{\cdot\cdot a}_{cb} = \bar{T}^{\cdot\cdot a}_{cb} + 2Q^{\cdot\cdot a}_{[cb]}, \tag{59}$$

where $\bar{T}^{\cdot\cdot a}_{cb}$ is the torsion of the crystal connection discussed in section 5.1 [16, 19, 21]. The components of the Riemann–Christoffel curvature tensor $\hat{R}^{\cdot\cdot\cdot a}_{bcd}$ are, from (28) and (55),

$$\hat{R}_{[ab]cd} = 2\hat{\nabla}_{[c}Q_{d][ba]} + \hat{T}^{\cdot\cdot e}_{cd}Q_{e[ba]}, \quad \hat{R}_{(ab)cd} = 2\hat{\nabla}_{[c}Q_{d](ab)} + \hat{T}^{\cdot\cdot e}_{cd}Q_{e(ab)} = 0. \tag{60}$$

Thus we see that the curvature is limited to nine independent components, i.e. $\hat{R}_{abcd} = \hat{R}_{[ab][cd]}$.

Consider a Burgers circuit c in the current configuration, enclosing area a comprised of oriented elements $\mathbf{n}da$. A total Burgers vector accounting for incompatibility induced by torsion and curvature may be written as [40, 44, 45]

$$B^a \equiv \frac{1}{2}\varepsilon^{dbc}\int_a \left(\hat{T}^{\cdot\cdot a}_{bc} - \hat{R}^{\cdot\cdot\cdot a}_{ecb}x^e\right)n_d da = B^a_T + B^a_R, \tag{61}$$

where $2B^a_T \equiv \varepsilon^{dbc}\int_a \hat{T}^{\cdot\cdot a}_{bc}n_d da$ describes the closure failure of c and $2B^a_R \equiv \varepsilon^{bdc}\int_a \hat{R}^{\cdot\cdot\cdot a}_{ecb}x^e n_d da$ measures the change in direction of position vector x^e upon parallel transport about c with respect to the connection $\hat{\mathbf{\Gamma}}$. Equation (61) reduces to (42) when disclinations are absent (i.e. when $\hat{T}^{\cdot\cdot a}_{bc} = \bar{T}^{\cdot\cdot a}_{bc}$, $Q^{\cdot\cdot a}_{bc} = 0$, and $\hat{R}^{\cdot\cdot\cdot a}_{bcc} = 0$) . We can re-write (61) in terms of the second rank geometrically necessary dislocation tensor $\boldsymbol{\alpha}$ and second rank geometrically necessary disclination tensor $\boldsymbol{\theta}$, each referred to the spatial configuration B:

$$B^a = \int_a \left(\alpha^{ad} + C^{L-1af}\varepsilon_{fgb}\theta^{gd}x^b\right)n_d da, \tag{62}$$

where

$$2\alpha^{ad} \equiv \varepsilon^{dbc}\hat{T}^{\cdot\cdot a}_{bc}, \quad 4\theta^{gd} \equiv \varepsilon^{gba}\varepsilon^{dce}\hat{R}_{abce}. \tag{63}$$

Figure 6 illustrates the total Burgers vector $\mathbf{B} = \mathbf{B_T} + \mathbf{B_R}$ introduced in equation (62) in terms of parallel transport of a lattice director vector $\mathbf{d}_a$ about an incompatibility circuit c [40]. When viewed from the standpoint of a Volterra process [41], one can imagine the body in figure 6 to consist of the superposition of a single edge dislocation (producing the incompatibility $\mathbf{B_T}$) and a single wedge disclination (producing the incompatibility $\mathbf{B_R}$).

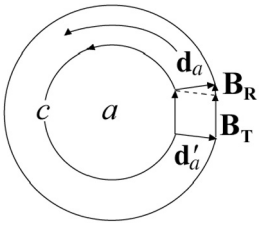

Figure 6. Burgers vector with contributions from dislocations ($\mathbf{B_T}$) and disclinations ($\mathbf{B_R}$).

Defect tensors $\boldsymbol{\alpha}$ and $\boldsymbol{\theta}$ contain information enabling us to fully reconstruct $\hat{\mathbf{T}}$ and $\hat{\mathbf{R}}$:

$$\hat{T}^{\cdot\cdot a}_{cb} = \hat{T}^{\cdot\cdot a}_{[cb]} = \varepsilon_{cbd}\alpha^{ad}, \quad \hat{R}_{abcd} = \hat{R}_{[ab][cd]} = \varepsilon_{bae}\varepsilon_{cdf}\theta^{ef}. \tag{64}$$

The tensors of (63) are also related to the summed contributions of discrete crystal defects as

$$\boldsymbol{\alpha} = \sum_j \rho^j \mathbf{b}^j \otimes \boldsymbol{\xi}^j, \quad \boldsymbol{\theta} = \sum_k \eta^k \boldsymbol{\omega}^k \otimes \boldsymbol{\zeta}^k, \tag{65}$$

with ρ^j, $\mathbf{b}^j$, and $\boldsymbol{\xi}^j$ the *net* scalar dislocation line density, Burgers vector, and unit tangent line, respectively, for dislocation population j, and with η^k, $\boldsymbol{\omega}^k$, and $\boldsymbol{\zeta}^k$ the net scalar disclination line density, Frank vector, and unit tangent line, respectively, for disclination population k.

Notice that $\boldsymbol{\alpha}$ and $\boldsymbol{\theta}$ do not account for curved defect segments and combinations of defect lines that do not contribute to a net Burgers vector. This is evident when (65) is written in terms of positively- and negatively-signed defect populations [29]:

$$\boldsymbol{\alpha} = \sum_j \left(\rho^j_+ - \rho^j_-\right)\mathbf{b}^j_+ \otimes \boldsymbol{\xi}^j, \quad \boldsymbol{\theta} = \sum_k \left(\eta^k_+ - \eta^k_-\right)\boldsymbol{\omega}^k_+ \otimes \boldsymbol{\zeta}^k, \tag{66}$$

where $\mathbf{b}^j_+ = -\mathbf{b}^j_-$ and $\boldsymbol{\omega}^k_+ = -\boldsymbol{\omega}^k_-$. It is emphasized that while the *net* defect densities of (63), (65) and (66) represent incompatibility, the *total* mobile defect densities contribute to the rate of plastic deformation (to $\dot{\mathbf{F}}^{\mathbf{p}}$), the latter which may be nonzero even in the absence of net defect densities, as would occur under conditions of homogeneous plastic flow (e.g. when $\rho^j_+ = \rho^j_-$). We use the qualifiers 'net', 'geometrically necessary', and 'non-redundant' interchangeably to describe defect densities producing nonzero incompatibility.

Linearized compatibility equations for the defect density tensors of (63) follow from identities of Bianchi and Schouten (*cf.* [55]), expressed in Cartesian coordinates as

$$\hat{T}^{\cdot\cdot a}_{[bc,\,d]} = \hat{R}^{\cdot\cdot a}_{[bcd]} \rightarrow \left(C^L\alpha\right)^{\cdot b}_{a,\,b} = \varepsilon_{abc}\theta^{bc}, \quad \hat{R}^{\cdot\cdot a}_{b[cd,\,e]} = 0 \rightarrow \theta^{ab}{}_{,b} = 0. \tag{67}$$

In a small-strain formulation that employs additive elastoplastic strains and rotation gradients, De Wit [48] inferred from equations analogous to (67) that disclinations may act as sources/sinks for dislocations, and that disclination lines cannot end

abruptly within a crystal. When disclinations are absent, the first of (67) depicts a divergence-free dislocation density tensor, meaning that dislocations cannot start or end within the crystal.

5.3. *Point defects*

We focus attention now upon a geometric representation of uniformly-distributed, isotropic point defects. The same connection $\hat{\mathbf{\Gamma}}$ listed in equation (22) is used, but the form of $\mathbf{Q}$ is restricted as follows [45]:

$$\hat{\Gamma}^{..a}_{cb} \equiv F^{La}_{.\bar{\alpha}} F^{L-1\bar{\alpha}}_{.b,c} + Q^{..a}_{cb} = \bar{\Gamma}^{..a}_{cb} + Q_c \delta^a_b, \quad Q^{..a}_{cb} = Q_c \delta^a_b, \quad Q_{cba} = Q_c C^L_{ba}. \tag{68}$$

From (68), the contribution from point defects to the derivative $\hat{\nabla}_c \mathbf{d}_a dx^c$ is given by $Q^{..b}_{ca} dx^c = \delta^b_a Q_c dx^c$, a pure stretch. The connection is non-metric since, by (24) and (68),

$$\hat{\nabla}_c C^L_{ab} = -2Q_{c(ab)} = -2Q_c C^L_{ab}, \tag{69}$$

meaning physically that vacancies, interstitials, or micro-voids alter the counting of atomic steps in the crystal [102]. The torsion becomes, upon substitution of (68) into (25),

$$\hat{T}^{..a}_{cb} \equiv \hat{\Gamma}^{..a}_{cb} - \hat{\Gamma}^{..a}_{bc} = \bar{T}^{..a}_{cb} + Q_c \delta^a_b - Q_b \delta^a_c, \tag{70}$$

thereby including a contribution to the non-redundant dislocation density $2\alpha^{ad} \equiv \varepsilon^{dbc} \hat{T}^{..a}_{bc}$ from the crystal connection $\bar{\Gamma}^{..a}_{cb}$ and a contribution from micromorphic contraction/expansion in the form $Q_b \delta^a_c - Q_c \delta^a_b$. From equation (27), the Riemann–Christoffel curvature tensor becomes simply

$$\hat{R}^{...a}_{bcd} = \left(2\hat{\nabla}_{[c} Q_{d]} + \hat{T}^{..e}_{cd} Q_e\right)\delta^a_b = 2Q_{[d,c]}\delta^a_b \underbrace{-\left(2\hat{\Gamma}^{..e}_{[cd]} Q_e - \hat{T}^{..e}_{cd} Q_e\right)\delta^a_b}_{=0} = 2\delta^a_b Q_{[d,c]}. \tag{71}$$

Upon parallel transport around a current configuration circuit c, a lattice director vector $\mathbf{d}_a$ changes by an amount $\Delta\mathbf{d}_a$ as follows in the presence of a non-vanishing curvature tensor $\hat{R}^{...a}_{bcd}$ [44, 55, 56]:

$$\Delta\mathbf{d}_a \equiv \mathbf{d}'_a - \mathbf{d}_a = \frac{1}{2}\int_a \hat{R}^{...b}_{acd}\mathbf{d}_b dx^c \wedge dx^d = -\mathbf{d}_a \int_a Q_{[c,d]} dx^c \wedge dx^d, \tag{72}$$

where we have used (71). From the last of (72), we see that the vector $\mathbf{d}_a$ is unchanged in direction upon completion of the circuit c; its components merely undergo stretch or reduction.

Recall that the micromorphic variable $\mathbf{Q}$ represents additional degrees-of-freedom at the microscale for capturing the effects of defects on spatial gradients of the lattice directors. Accompanying $\mathbf{Q}$ at the macroscale is the contribution of these defects to $\mathbf{F}$ of (17). The contribution of isotropic defects may be written in terms of our $\mathbf{F}^{\mathbf{i}}$ term, neglecting here the contributions of anisotropic residual lattice deformation:

$$\mathbf{F}^{\mathbf{i}} = \left(\upsilon \delta^{\alpha}_{.\bar{\beta}}\right)\mathbf{g}_\alpha \otimes \mathbf{g}^{\bar{\beta}}, \tag{73}$$

where the scalar υ is given by

$$\upsilon = (1-\phi)^{-1/3}, \tag{74}$$

where ϕ will be defined shortly. Consider differential volume elements $d\tilde{V} \in \tilde{\boldsymbol{B}}$ and $d\bar{V} \in \bar{\boldsymbol{B}}$. The relationship between these volume elements, upon appealing to (73) and (74), is then

$$d\tilde{V} = J^{i} d\bar{V} = \det \mathbf{F}^{\mathbf{i}} \sqrt{\det \tilde{\mathbf{g}} / \det \mathbf{g}}\, d\tilde{V} = d\bar{V}(1-\phi)^{-1}, \tag{75}$$

upon assuming coincident coordinate frames on $\tilde{\boldsymbol{B}}$ and $\bar{\boldsymbol{B}}$ (and thus equivalent metric tensors $\tilde{\mathbf{g}}$ and $\mathbf{g}$). Equation (75) then provides the definition for the scalar ϕ:

$$\phi = \left(d\tilde{V} - d\bar{V}\right)/d\tilde{V}. \tag{76}$$

When microvoids or interstitials are considered, ϕ is the fraction of defects in the intermediate configuration, per intermediate configuration volume [95]:

$$\phi\, d\tilde{V} = \left(N^{+}\tilde{V}^{+} + d\bar{V}\right) - d\bar{V} = N^{+}\tilde{V}^{+}, \tag{77}$$

where N^{+} and $\tilde{V}^{+}$ are the number of defects and the volume of each defect, respectively, within the local volume element $d\tilde{V}$, in configuration $\tilde{\boldsymbol{B}}$. For an isotropic distribution of vacancies, there is a net *decrease* in volume due to $\mathbf{F}^{\mathbf{i}}$, and we have [96]

$$\phi\, d\tilde{V} = \left(-N^{-}\tilde{V}^{-} + d\bar{V}\right) - d\bar{V} = -N^{-}\tilde{V}^{-}, \tag{78}$$

with N^{-} the number of vacancies within volume element $d\tilde{V}$, each inducing reduction $\tilde{V}^{-}$.

6. Summary

Our theory is founded upon two major assumptions, the first being a three-term decomposition of the average deformation gradient for a crystal element (see also equation (17)):

$$\mathbf{F} = \underbrace{\mathbf{F}^{\mathbf{e}}\mathbf{F}^{\mathbf{i}}}_{\mathbf{F}^{L}}\mathbf{F}^{\mathbf{p}}, \tag{79}$$

with the $\mathbf{F}^{\mathbf{i}}$ term, non-standard in the usual theories from the literature (*cf.* [97]), accounting for the presence of defects that affect the average lattice arrangement and internal residual stresses within the crystalline volume element (see figure 2). Also in (79) are the elastic deformation $\mathbf{F}^{\mathbf{e}}$ representing both the recoverable lattice stretch associated with the average applied stress acting on the element and rigid-body rotations of the lattice, as well as the plastic deformation $\mathbf{F}^{\mathbf{p}}$ accounting for the partition of fluxes of mobile defects that leaves the lattice unperturbed. The total lattice deformation is written as $\mathbf{F}^{L}$. The second major assumption is an additive decomposition of a linear connection describing spatial gradients of the slip directions and lattice director vectors between neighboring crystalline elements

(i.e. the microscopic description). Christoffel symbols of this connection, introduced in equation (22), may be written as

$$\hat{\Gamma}^{\cdot\cdot a}_{cb} = \underbrace{F^{La}_{\tilde{\alpha}} F^{L-1\tilde{\alpha}}_{b,\,c}}_{\substack{\text{crystal}\\ \text{connection}\\ (GNDs)}} + \underbrace{C^{L-1ad} Q_{c[bd]}}_{\substack{\text{micro-rotation}\\ (\text{disclinations})}} + \underbrace{\delta^a_b Q_c}_{\substack{\text{micro-expansion}\\ (\text{isotropic point defects})}} + \underbrace{C^{L-1ad}\left(Q_{c(bd)} - Q_c C^L_{bd}\right)}_{\substack{\text{micro-strain}\\ (\text{Somigliana dislocations})}}, \quad (80)$$

where the first term on the right side describes gradients of the director vectors due to first-order gradients in the average lattice deformation tensor $\mathbf{F}^L$, following Bilby *et al*. [19], as discussed in section 5.1. The micromorphic variable $\mathbf{Q}$ (*cf*. [45, 48]) participates in the remaining three terms on the right of (80): a micro-rotation associated with disclinations, as discussed in section 5.2, an isotropic micromorphic expansion associated with point defects, discussed in section 5.3, and a general micromorphic strain that may be used to represent arbitrary lattice director deformations when superposed with the other terms in (80). Dislocation and disclination density tensors then follow from the torsion and curvature, respectively, of the connection (80), the latter vanishing when the variable $\mathbf{Q}$ vanishes. Our theory is unique from others in the literature via its combination of the three-term deformation decomposition (79) with the additive connection for geometrically-necessary defects (80). Note that it is possible to describe defect kinematics (e.g. construct the dislocation and disclination density tensors) without decomposing the lattice deformation $\mathbf{F}^L$ into distinct recoverable and residual terms. For example, Minagawa [45, 46] invoked a connection similar to (80), but used only a single elastic lattice deformation map, amounting in essence to a two-term deformation gradient decomposition. However, we find our three-term decomposition more realistic than the usual two-term decomposition from the viewpoint of developing constitutive relations, with only the recoverable portion $\mathbf{F}^{\mathbf{e}}$ of the lattice deformation $\mathbf{F}^L$ acting as a thermodynamic force conjugate to the externally applied stress [67].

In summary, we present table 1, which depicts the classifications of the affine geometries corresponding to crystal defects in finite elastoplasticity, following terminology of our section 2 and motivated by Steinmann [6]. Figure 7 is a two-dimensional idealization of a crystalline element in the spatial configuration containing the lattice defects listed in table 1. We remark that in many figures in this paper, simple cubic lattices have been used to illustrate key concepts, as this crystal structure is easiest to visualize. Our framework has been developed with the primary intention of describing engineering metals that deform by dislocation glide, most typically exhibiting a Bravais lattice structure and most often realized in a face-centered-cubic, body-centered-cubic, or hexagonal close-packed arrangement. The concepts forwarded herein are most naturally applied to cubic lattices, wherein the director vectors of (18) may be assigned parallel to the primitive translation vectors of the lattice. The framework is valid for crystal structures of lower symmetry (e.g. hexagonal) so long as the Cauchy–Born rule (*cf*. [103]) applies for the elastic deformation of the interatomic bond vectors. In such cases, while the directors of relations (18) assigned to each crystal volume element are not parallel to the physical edges of the unit cell of the lattice, they are assumed to fully characterize the stretch and rotation of the interatomic vectors comprising the primitive cell. On the other hand, for more exotic structures wherein the recoverable deformation is non-uniform

Table 1. Geometric classifications, kinematic quantities, and corresponding crystal defects.

Geometry	Torsion	Curvature	Metric	Defects
Euclidean ($\bar{\boldsymbol{B}}$ admits holonomic coordinates)	$\hat{\mathbf{T}} = \mathbf{0}$	$\hat{\mathbf{R}} = \mathbf{0}$	$\hat{\nabla}\mathbf{C}^L = \mathbf{0}$ (yes)	Statistically stored dislocations (SSDs)* figure 7a
Cartan and non-Riemannian (e.g. $\hat{\mathbf{\Gamma}} = \bar{\mathbf{\Gamma}}$)	$\hat{\mathbf{T}} \neq \mathbf{0}$	$\hat{\mathbf{R}} = \mathbf{0}$	$\hat{\nabla}\mathbf{C}^L = \mathbf{0}$ (yes)	Geometrically necessary dislocations (GNDs) figure 7b
Riemannian and symmetric	$\hat{\mathbf{T}} = \mathbf{0}$	$\hat{\mathbf{R}} \neq \mathbf{0}$	$\hat{\nabla}\mathbf{C}^L = \mathbf{0}$ (yes)	Disclinations
Metric, Cartan, and Riemannian	$\hat{\mathbf{T}} \neq \mathbf{0}$	$\hat{\mathbf{R}} \neq \mathbf{0}$	$\hat{\nabla}\mathbf{C}^L = \mathbf{0}$ (yes)	GNDs and disclinations figure 7c
Non-metric, Cartan, and Riemannian	$\hat{\mathbf{T}} \neq \mathbf{0}$	$\hat{\mathbf{R}} \neq \mathbf{0}$	$\hat{\nabla}\mathbf{C}^L \neq \mathbf{0}$ (no)	All types of defects (e.g. point and line defects) figure 7d

*Admissible defects for all geometries in table 1. However, all dislocations are geometrically necessary when considered in isolation; collections of SSDs produce no net Burgers vector and no net torsion tensor.

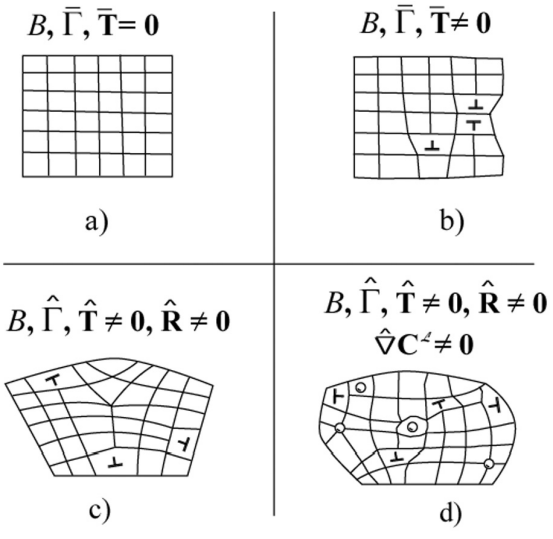

Figure 7. Current configuration lattices accompanying table 1: (a) Euclidean space, (b) Cartan space, (c) Cartan and Riemannian space, (d) general non-metric space.

within the unit cell, additional degrees of freedom not included in our theory are required—see for example the couple stress-based treatment of diamond cubic-structured silicon by Garikipati [98].

6. Conclusions

A comprehensive and rigorous theoretical framework for the finite deformation kinematics of lattice defects in crystalline materials has been presented.

The framework includes a three-term multiplicative decomposition of the deformation gradient, with terms accounting for recoverable elasticity, residual lattice deformation due to defect populations, and plastic deformation resulting from defect fluxes. Also invoked is an additional micromorphic variable representing additional degrees-of-freedom associated with lattice defects other than conventional translational dislocations, such as disclinations, point defects, and most generally, Somigliana dislocations. Our treatment has been purely kinematic in nature; accompanying thermodynamics and kinetics remain to be addressed in future work.

Acknowledgements

JDC thanks the Weapons and Materials Research Directorate of the US Army Research Laboratory. DJB is grateful for support of Sandia National Laboratories under US Department of Energy contract no. DE-AC04-94AL85000. DLM acknowledges support of AFOSR (MURI (1606U81) and F49620-01-1-0034).

References

[1] G.A. Maugin, *Material Inhomogeneities in Elasticity* (Chapman and Hall, London, 1993).
[2] G.A. Maugin, Appl. Mech. Rev. **48** 213 (1995).
[3] G.A. Maugin, J. Elast. **71** 81 (2003).
[4] K.C. Le and H. Stumpf, Proc. R. Soc. Lond. A **452** 359 (1996).
[5] K.C. Le and H. Stumpf, Int. J. Eng. Sci. **34** 339 (1996).
[6] P. Steinmann, Int. J. Eng. Sci. **34** 1717 (1996).
[7] D.G.B. Edelen and D.C. Lagoudas, Int. J. Eng. Sci. **37** 59 (1999).
[8] A. Acharya and J.L. Bassani, J. Mech. Phys. Solids **48** 1565 (2000).
[9] B. Svendsen, Acta Mech. **152** 49 (2001).
[10] J.D. Eshebly, Phil. Trans. R. Soc. Lond. **244** 87 (1951).
[11] J.D. Eshelby, *Solid State Physics*, vol. 3, edited by F. Séitz and D. Turnbull (Academic Press, New York, 1956), pp. 79–144.
[12] F.R.N. Nabarro, Proc. R. Soc. Lond. A **398** 209 (1985).
[13] E. Kröner, Mat. Sci. Forum **123/125** 447 (1993).
[14] M.E. Gurtin, Arch. Rat. Mech. Anal. **131** 67 (1995).
[15] B.A. Bilby, L.R.T. Gardner and A.N. Stroh, in *Proceedings 9th International Congress on Applied Mechanics*, vol. 8, Université de Bruxelles (1957), pp. 35–44.
[16] E. Kröner, Arch. Rat. Mech. Anal. **4** 273 (1960).
[17] C. Eckart, Phys. Rev. **73** 373 (1948).
[18] K. Kondo, *Proceedings 2nd Japan Congress Applied Mechanics* (Japan National Committee for Theoretical and Applied Mechanics, Science Council of Japan, Tokyo, 1953), pp. 41–47.
[19] B.A. Bilby, R. Bullough and E. Smith, Proc. R. Soc. Lond. A **231** 263 (1955).
[20] A. Einstein, Sitz. Preuβ. Akad. 217 (1928).
[21] W. Noll, Arch. Rat. Mech. Anal. **27** 1 (1967).
[22] K.R. Rajagopal and A.R. Srinivasa, Int. J. Plast **14** 945 (1998).
[23] P. Cermelli and M.E. Gurtin, J. Mech. Phys. Solids **49** 1539 (2001).
[24] J.E. Marsden, S. Pekarsky, S. Shkoller, *et al.*, J. Geom. Phys. **38** 253 (2001).
[25] D.C. Lagoudas and D.G.B. Edelen, Int. J. Eng. Sci. **27** 411 (1989).
[26] D.G.B. Edelen, Int. J. Eng. Sci. **34** 81 (1996).
[27] M.F. Ashby, Phil. Mag. **21** 399 (1970).
[28] R.W. Lardner, Z. Agnew. Math. Phys. **20** 514 (1969).

[29] R.W. Werne and J.M. Kelly, Int. J. Eng. Sci. **16** 951 (1978).
[30] J.F. Nye, Acta Metall. **1** 153 (1953).
[31] F. Kroupa, Czech. J. Phys. **12** 191 (1962).
[32] E. Kröner, J. Math. Phys. **42** 27 (1963).
[33] E. Kröner, Rheol. Acta **12** 374 (1973).
[34] R. Bullough and B.A. Bilby, Proc. Phys. Soc. Lond. B **69** 1276 (1956).
[35] M.J. Marcinkowski and K. Sadananda, Acta Crystallogr. A **31** 280 (1975).
[36] C.S. Hartley and D.L.A. Blachon, J. Appl. Phys. **49** 4788 (1978).
[37] P. Cermelli and M.E. Gurtin, Acta Metall. Mater. **42** 3349 (1994).
[38] P. Dłużewski, Mech. Mater. **22** 23 (1996).
[39] K. Kondo, J. Japan Soc. Appl. Mech. **2** 146 (1949).
[40] K. Kondo, Int. J. Eng. Sci. **2** 219 (1964).
[41] V. Volterra, Ann. Ecole Norm. Sup. Paris **24** 401 (1907).
[42] F.R.N. Nabarro, *Theory of Crystal Dislocations* (Oxford University Press, 1967).
[43] K.H. Anthony, Arch. Rat. Mech. Anal. **39** 43 (1970).
[44] R.W. Lardner, Arch. Mech. **25** 911 (1973).
[45] S. Minagawa, Arch. Mech. **31** 783 (1979).
[46] S. Minagawa, Int. J. Eng. Sci. **19** 1705 (1981).
[47] S. Amari, Int. J. Eng. Sci. **19** 1581 (1981).
[48] R. De Wit, Int. J. Eng. Sci. **19** 1475 (1981).
[49] R.J. Asaro, Int. J. Eng. Sci. **13** 271 (1976).
[50] C. Teodosiu, Int. J. Eng. Sci. **19** 1563 (1981).
[51] R.B. Pęcherski, Arch. Mech. **35** 257 (1983).
[52] R.B. Pęcherski, Eng. Fract. Mech. **21** 767 (1985).
[53] E. Kröner, *Dislocation Modelling of Physical Systems*, edited by M.F. Ashby, R. Bullough, C.S. Hartley, *et al.* (Pergamon Press, Oxford, 1980), pp. 285–303.
[54] E. Kröner, *The Structure and Properties of Crystal Defects*, edited by V. Paidar and L. Lejček (Elsevier, Amsterdam, 1983), pp. 357–369.
[55] J.A. Schouten, *Ricci Calculus*, second edition (Springer, Berlin, 1954).
[56] C.-C. Wang and C. Truesdell, *Introduction to Rational Elasticity* (Noordhoff, Leyden, 1973).
[57] J.E. Marsden and T.J.R. Hughes, *Mathematical Foundations of Elasticity* (Dover, New York, 1983).
[58] L.P. Eisenhart, *Riemannian Geometry* (Princeton University Press, Princeton, 1926).
[59] W.M. Boothby, *An Introduction to Differentiable Manifolds and Riemannian Geometry*, second edition (Academic Press, Boston, 1986).
[60] H. Rund, *The Differential Geometry of Finsler Spaces* (Springer, Berlin, 1959).
[61] H. Stumpf and U. Hoppe, Z. Angew. Math. Mech. **77** 327 (1997).
[62] E. Cartan, Compt. Rend. **174** 593 (1922).
[63] B. Hou and B. Hou, *Differential Geometry for Physicists* (World Scientific, Singapore, 1997).
[64] C. Teodosiu, Rev. Roum. Sci. Technol. Méc. Appl. **12** 961 (1967).
[65] J.C. Simo and M. Ortiz, Comp. Methods Appl. Mech. Eng. **49** 221 (1985).
[66] J.D. Clayton, D.J. Bammann and D.L. McDowell, Int. J. Non-Linear Mech. **39** 1039 (2004).
[67] J.D. Clayton, D.L. McDowell and D.J. Bammann, Int. J. Eng. Sci. **42** 427 (2004).
[68] D.A. Hughes, N. Hansen and D.J. Bammann, Scripta Mater. **48** 147 (2003).
[69] P. Müllner and A.E. Romanov, Scripta Metall. Mater. **31** 1657 (1994).
[70] K.R. Rajagopal and A.R. Srinivasa, Z. Angew. Math. Phys. **55** 1074 (2004).
[71] J.D. Clayton and D.L. McDowell, Int. J. Plast. **19** 1401 (2003).
[72] J. Kratochvíl, in *Foundations of Plasticity*, edited by A. Sawzcuk (Noordhoff, Warsaw, 1972), pp. 401–415.
[73] A.C. Eringen and W.D. Claus Jr, in *Fundamental Aspects of Dislocation Theory*, edited by J.A. Simmons, R. de Wit and R. Bullough, vol. 2, (U.S. Government Printing Office, Gaithersburg, MD, 1970), pp. 1023–1040.

[74] R.W. Lardner, *Mathematical Theory of Dislocations and Fracture* (University of Toronto Press, Great Britain, 1974).
[75] P.M. Nagdhi and A.R. Srinivasa, Phil. Trans. R. Soc. Lond. A **345** 425 (1993).
[76] J. Mandel, Int. J. Solids Struct. **9** 725 (1973).
[77] C.S. Hartley, Phil. Mag. **83** 3783 (2003).
[78] M. Seefeldt, Rev. Adv. Mater. Sci. **2** 44 (2001).
[79] C. Somigliana, Rend. R. Acc. Lincei, Ser. 5 **23** 463 (1914).
[80] J.M. Burgers, Proc. Kon. Nederl. Akad. Wetensch. **42** 293 (1939).
[81] F.C. Frank, Disc. Faraday Soc. **25** 19 (1958).
[82] C. Teodosiu and F. Sidoroff, Int. J. Eng. Sci. **14** 713 (1976).
[83] A.E. Romanov, Phys. Scripta T **49** 427 (1993).
[84] J.C.M. Li, Surf. Sci. **31** 12 (1972).
[85] W. Bollmann, Mater. Sci. Eng. A **136** 1 (1991).
[86] J.C.M. Li and J.T. Gilman, J. Appl. Phys. **41** 4248 (1970).
[87] D.A. Konstantinidis and E.C. Aifantis, Nano Mater. **10** 1111 (1998).
[88] O.A. Shenderova and D.W. Brenner, Phys. Rev. B **60** 7053 (1999)
[89] A.A. Nazarov, O.A. Shenderova and D.W. Brenner, Phys. Rev. B **61** 928 (2000).
[90] T. Mura, *Micromechanics of Defects in Solids*, first edition (Nijhoff, Dordrecht, 1982).
[91] L.M. Zubov, *Nonlinear Theory of Dislocations and Disinclinations in Elastic Bodies* (Springer, Berlin, 1997).
[92] J.C.M. Li, Acta Metall. **8** 563 (1960).
[93] E. Kröner and D.C. Lagoudas, Int. J. Eng. Sci. **30** 47 (1992).
[94] M. Lazar and G.A. Maugin, J. Mech. Phys. Solids **52** 2285 (2004).
[95] D.J. Bammann and E.C. Aifantis, Nucl. Eng. Des **116** 355 (1989).
[96] E. Kröner, Int. J. Theo. Phys. **29** 1219 (1990).
[97] E.H. Lee, J. Appl. Mech. **36** 1 (1969).
[98] K. Garikipati, J. Mech. Phys. Solids **51** 1189 (2003).
[99] B.A. Bilby and E. Smith, Proc. R. Soc. Lond. A **232** 481 (1956).
[100] A. Acharya and J.L. Bassani, *Plastic and Fracture Instabilities in Materials*, AMD vol. 200/MD vol. 57, edited by N. Ghoniem (ASME, New York, 1995), pp. 75–80.
[101] C. Truesdell and W. Noll, *The Non-Linear Field Theories of Mechanics*, second edition (Springer, Berlin, 1965).
[102] E. Kröner, Int. J. Solids Struct. **29** 1849 (1992).
[103] J.L. Ericksen, *Phase Transformations and Material Instabilities in Solids* (Academic Press, New York, 1984), pp. 61–77.

NO. OF
COPIES ORGANIZATION

1 (PDF ONLY) DEFENSE TECHNICAL INFORMATION CTR
DTIC OCA
8725 JOHN J KINGMAN RD
STE 0944
FORT BELVOIR VA 22060-6218

1 US ARMY RSRCH DEV & ENGRG CMD
SYSTEMS OF SYSTEMS INTEGRATION
AMSRD SS T
6000 6TH ST STE 100
FORT BELVOIR VA 22060-5608

1 INST FOR ADVNCD TCHNLGY
THE UNIV OF TEXAS
AT AUSTIN
3925 W BRAKER LN
AUSTIN TX 78759-5316

1 DIRECTOR
US ARMY RESEARCH LAB
IMNE ALC IMS
2800 POWDER MILL RD
ADELPHI MD 20783-1197

3 DIRECTOR
US ARMY RESEARCH LAB
AMSRD ARL CI OK TL
2800 POWDER MILL RD
ADELPHI MD 20783-1197

ABERDEEN PROVING GROUND

1 DIR USARL
AMSRD ARL CI OK TP (BLDG 4600)

NO. OF
COPIES ORGANIZATION

ABERDEEN PROVING GROUND

30 DIR USARL
AMSRD ARL CI HC
P CHUNG
C CORNWELL
AMSRD ARL WM
M FERMEN COKER
T WRIGHT
J MCCAULEY
AMSRD ARL WM MA
W NOTHWANG
AMSRD ARL WM TA
S SCHOENFELD
AMSRD ARL WM TD
S BILYK
T BJERKE
D CASEM
J CLAYTON (10 CPS)
D DANDEKAR
M GREENFIELD
Y HUANG
K IYER
B LOVE
M RAFTENBERG
E RAPACKI
M SCHEIDLER
S SEGLETES
T WEERASOORIYA

INTENTIONALLY LEFT BLANK.